The background of the slide is a microscopic image showing several hydrogel-based edible barcodes. These barcodes are shaped like the letters 'T', 'U', and 'L'. They have a dark, porous, and textured appearance, suggesting a complex internal structure. The barcodes are arranged in a grid-like pattern on a light-colored, textured surface.

Developing Edible Barcodes from Hydrogels

A study on the influence of drying

Pavithra Vasanth Bailey
4626249

Technische Universiteit Delft

DEVELOPING EDIBLE BARCODES FROM HYDROGELS

A STUDY ON THE INFLUENCE OF DRYING

by

Pavithra Vasanth Bailey

4626249

in partial fulfillment of the requirements for the degree of

Master of Science
in Chemical Engineering

at the Delft University of Technology,
to be defended publicly on Monday, May 28 2018 at 11:00 am.

Supervisor:	Dr. H. Burak Eral	TU Delft
Thesis committee:	Prof. Dr. Antoine van der Heijden, Dr. Eduardo Mendes	TU Delft TU Delft

This thesis is confidential and cannot be made public until May 28, 2018.

An electronic version of this thesis is available at <http://repository.tudelft.nl/>.

Cover image represents a prototype of 8% w/w alginate hydrogel barcode.

Image credits: Yesaswini Katragadda and Pavithra Vasanth Bailey.

Report Number: P&E-2743

“The most beautiful experience we can have is the mysterious. It is the fundamental emotion that stands at the cradle of true art and true science”

-Albert Einstein

ABSTRACT

Counterfeiting of food and pharmaceutical products, albeit a more serious issue in developing countries is, however, omnipresent. Therefore, there is an ever-growing need for anticounterfeiting measures to address this challenge. Currently, the existing overt and covert anticounterfeiting measures are more prevalent on the packaging of such products. While such measures are helpful to a certain extent, they are however, easier to by-pass with re-used authentic packaging, fake barcodes and duplicate product numbering. Furthermore, advanced research and new innovations have indicated that it is also possible to have additional levels of security by incorporating similar measures into or on the product itself. Although these novel anticounterfeiting measures offer a unique opportunity to safeguard the customer's interest at best, they present certain challenges. Some of these include biocompatibility of the materials and the need for them to be in compliance with regulatory organizations. However, overcoming these challenges confronts the issue directly. In this work, the approach is to develop a proof of concept of entirely edible barcodes from naturally available and/or food grade materials such as sodium alginate. This study also focuses on the influence of drying on the macroscopic structure of such barcodes. The barcodes are produced by physically cross-linking the polymer in specific moulds, converting them into a hydrogel barcode in itself. Altogether, this work provides a qualitative understanding that such a concept can be developed and that the significant structural changes upon drying is not exclusively governed by the concentration of sodium alginate.

Keywords: anticounterfeiting, hydrogel, edible barcode, sodium alginate, drying, thermogravimetric analysis.

*Pavithra Vasanth Bailey
Delft, May 2018*

LIST OF ABBREVIATIONS

1D	One-Dimensional
2D	Two-Dimensional
3D	Three-Dimensional
ABS	Acrylonitrile Butadiene Styrene
ALG	Alginate hydrogel
CaCl ₂	Calcium Chloride
CaCO ₃	Calcium Carbonate
CAD	Computer-aided Design
DI water	Deionized water
DNA	Deoxyribonucleic acid
EDS	Energy Dispersive Spectroscopy
EDX	Energy Dispersive X-Ray
FDA	Food and Drug Administration
FFDCA	Federal Food, Drug, and Cosmetic Act
GDL	Glucono- δ -lactone
GRAS	Generally Regarded as Safe
HEPES	4-(2-hydroxyethyl)-1-piperazineethanesulfonic acid
IUPAC	International Union of Pure and Applied Chemistry
Na-Alg	Sodium Alginate
NaCl	Sodium Chloride
pH	Potential of hydrogen
PMMA	Poly(methyl methacrylate)
QR code	Quick Response Code
SEM	Scanning Electron Microscope
TGA	Thermogravimetric Analysis
WHO	World Health Organization
XRD	X-ray Diffraction

LIST OF TABLES

2.1	General advantages and limitations of hydrogels	7
3.1	Overview of chemicals utilized	12
4.1	Experimental results for curing of hydrogel in the 3D printed moulds	22
4.2	Dimensions for 6% w/w Na-Alg (20 mM CaCO ₃)	23
4.3	Dimensions for 6% w/w Na-Alg (40 mM CaCO ₃)	24
4.4	Change in dimensions for 8% w/w barcode	27
4.5	Change in dimensions for 10% w/w barcode	28

LIST OF FIGURES

2.1	Classification of Polymers	4
2.2	Classification of Polymers	6
2.3	Molecular structure of Alginate	9
2.4	Egg-box structure of Alginate	10
3.1	Schematic of experimental setup	13
3.2	3D polymer mould design	15
4.1	Metal stampers	17
4.2	6% w/w Na-Alg sample in rectangular metal stamper	18
4.3	6% w/w Na-Alg sample in circular stamper (poorly cured barcodes)	19
4.4	Deposits of 12% w/w Na-Alg (with HEPES) on circular metal stamper	20
4.5	Barcodes developed from 3D polymer mould	22
4.6	Drying of 6% w/w Na-Alg barcodes (20 mM CaCO ₃)	23
4.7	Drying of 6% w/w Na-Alg barcodes (20 mM CaCO ₃)	24
4.8	Deposits on hydrogel barcodes	25
4.9	Percentage of (water lost/initial water) vs Na-Alg concentration	26
4.10	Drying of 8% w/w Na-Alg barcode	27
4.11	Drying of 10% w/w Na-Alg barcode	28
6.1	Laser cut barcode on edible sheets	31
6.2	Deposits on the polymer mould	32
A.1	Artificially fingerprinted microparticle for a biomimetic fingerprint	37
B.1	TGA for 2% and 12% w/w Na-Alg	38
B.2	TGA for all concentrations of Na-Alg	39
B.3	Predicted curve for evaporation of water	39
B.4	Double exponential curve fit TGA data	40
B.5	Fitting parameters for the double exponential curve fit for TGA data	40
C.1	Normalized weight loss of ALG vs Time (for 20 mM CaCO ₃)	42
C.2	Normalized weight loss of ALG vs Time (for 40 mM CaCO ₃)	43
C.3	Mass balance (TGA)	44
C.4	Mass balance (20 mM CaCO ₃)	44
C.5	Mass balance (40 mM CaCO ₃)	45
C.6	Percentage of Na-Alg vs weight percentage of the sample after drying	45
C.7	Percentage of Na-Alg vs percentage of water lost (TGA)	46
C.8	Composite barcode	46
C.9	Metal stamper tests	47

CONTENTS

Abstract	iii
List of Abbreviations	v
List of Tables	vi
List of Figures	vii
1 Introduction	1
2 Theoretical Background	4
2.1 Polymers and Governing Terminologies	4
2.2 Hydrogels	5
2.3 Cross-linking of Hydrogels.	7
2.3.1 Chemically cross-linked gel	7
2.3.2 Physically cross-linked gel.	8
2.3.3 Generally Regarded as Safe (GRAS) Polymers	8
2.4 Sodium Alginate	8
2.4.1 Introduction	8
2.4.2 Structure	9
2.4.3 Advantages and Uses	10
2.5 Thesis Objectives	11
3 Materials and Methods	12
3.1 Materials	12
3.2 Synthesis of Alginate Hydrogels.	12
3.2.1 Preparation of Na-Alg Solutions	12
3.2.2 First Phase of Curing	12
3.2.3 Second Phase of Curing	13
3.3 Moulds for Curing of Hydrogel	14
3.3.1 Metal Stamper	14
3.3.2 3D Printed Polymer Mould	14
3.4 Post Processing	15
3.4.1 Drying.	15
3.4.2 Alterations in the protocol.	15
4 Results and Discussion	17
4.1 Moulds for curing of hydrogel.	17
4.1.1 Metal Stampers	17
4.1.2 3D Printed Polymer Mould	21
4.2 Drying Studies	23
4.3 Alterations in experimental protocol.	24
4.4 Further Drying Analysis	25
4.4.1 Effect of varying thickness on the barcodes post drying	27

5	Conclusions	29
6	Recommendations and Limitations	31
7	Acknowledgements	34
A	Buckling Instability	36
B	Thermogravimetric Study	38
C	Mass Balances, Supplementary Experiments & Figures	42
	Bibliography	48

1

INTRODUCTION

The food and pharmaceutical industries must comply with several stringent criteria in terms of quality at a global level [1]. This refers not only to the final product reaching the end consumers but to each step of the manufacturing process leading to the finished product. However, even in the 21st century, counterfeit products that are potentially harmful enter the market everyday, escalating the significance of public health and safety. The products that fall under this category include manufactured products of inferior quality [2, 3], i.e., adulterated products or products that alter their properties due to improper storage conditions [1, 4], and/or maintenance at various stages along the supply chain.

Within the pharmaceutical sector alone, counterfeiting is reaching a significant level, with statistics showing an estimate of approximately 10-30% of counterfeit products. The higher percentage of this reflects the current situation in developing countries, in Africa, parts of Asia and Latin America [5]. This statistic is an indication of the counterfeit medicines that are being sold in the market and 50% for those bought via the internet [5]. For instance, more than 30 Nigerian children died due to poisoned teething medicine that contained close to 90 ml of diethylene glycol per 100 ml of medicine [6]. Relatively startling incidents can also be found in the food industry. One such alarming example can be traced back to the milk powder scandal in China in 2008 where close to three hundred thousand children fell ill and six babies lost their lives due to substandard milk powder tainted with melamine [7, 8] (disguised as having higher protein content upon further testing [9]).

In order to address this underlying issue at hand, World Health Organization (WHO) has proposed and approved certain overt and covert anti-counterfeiting measures [10]. Holograms, security inks and films, on-product marking, invisible printing, and laser coding [10] are some examples among several other techniques. These methods are used to foster the safety of consumers and ensure that the end-to-end process are undertaken responsibly by the suppliers [11, 12].

As discussed previously, the percentage of counterfeit products entering the market is on the increase, [5] creating a growing need to improve the authentication technologies available. The melamine milk scandal [10] led to an extensive demand for European milk powder, consequently leading to a quintuple rise in the price, further posing a threat to the security of the export trading sector for such commodities [13]. As a direct consequence, research devoted to developing complex technologies which can be applied to adding security layers to these products are upcoming at a faster rate.

Numerous such applications are listed in literature, applying different mechanisms which aid in detecting authenticity of food and pharmaceutical products. Some of these are drug laden 3D QR codes directly from inkjet printing using upconversion (the process where

numerous low energy photons are converted to one single high energy photon) fluorescent nanoparticles [14] and 3D biodegradable labels as films fabricated from PMMA by means of laser engraving [15]. Some other examples found in literature include numerous applications using bioink based and the bioprintability of hydrogels for 1D, 2D and 3D configurations [16, 17] and multilayer printable microtaggants incorporating the mechanism of phase change of nanoparticles [18]. Similarly, chemical molecular tags [19], tracking of biological agents using coating methods [20] as well as DNA based taggants with encoded messages [21] and barcodes [22] have also been researched for application. The above mentioned research and more have directly led to commercialization of such devices for detecting authenticity, like TruTag®[23], Taaneh™[24], DNATrax™[25] and SafeTracers™[26]. Nevertheless, validation of the end product using these technologies demands for specific instrumentation at hand, such as a spectrometer or a polymerase chain reaction kit (PCR), slightly reducing the simplicity and convenience for the end customer [1].

A large number of the innovations found in literature follow the non-degradable route and/or contain toxic substances such as metallic and fluorescent nanoparticles. However, according to existing literature, biodegradable barcodes are exclusive to microfibrils from alginate and polylactic-*co*-glycolic acid [1].

A similar research recently done by Rehor *et al.* indicates that it is possible to have such a barcode which can be multi-functional, i.e., it can provide authentic information about a product as well as sensory information [1] based on the storage and handling of a particular product. The basic concept focuses on having one end of the barcode thicker than the other so that the sensory information can be picked up based on deformations (due to change in temperature) and photo-initiation in the barcode (change in pH due to microbial activity) [1]. While there is validation that this barcode can be functional, it however, works on the principle of free radical polymerization [1] which incorporates complex chemistry that is not yet suitable to be applied into products directly ingested or that is compatible with the human body.

The work discussed above provides direct inspiration and motivation for developing an edible barcode from biocompatible hydrogels. To the best of our knowledge, substantial literature is unavailable about the conceptualization of an edible barcode from hydrogels. Therefore, in an attempt to further enhance not only the simplicity but also the materials used in the existing technologies, the aim of this project is to develop a similar barcode that is entirely edible in itself.

Consequently, in the research presented in this thesis, the objective is to develop a barcode through experimental protocols that is complicated in terms of the skill set required for manufacturing such a barcode, making it difficult to replicate. However, simultaneously, it also aims at simpler chemistry by reducing the number of materials used to a minimum, providing maximum convenience to the end consumer.

Therefore, this research focuses on the study of behaviour of biocompatible hydrogels in the form of barcodes as a proof of concept, starting from the development stage and their structural changes influenced by post processing methods, such as drying.

The results presented in this thesis represent a preliminary effort in the direction to-

wards development of such a concept and provides a framework to further continue and improve the methodology. The long-term goal of the work presented in this thesis is to reach to a quantifiable end result with a working model which can be applied in the market, particularly in the food and pharmaceutical sector. One that makes use of simpler chemistry, is more compatible for ingestion and reduces the difficulty of identification by the end user.

THEORETICAL BACKGROUND

The theoretical background presented in this chapter includes some basic description about polymers, their classification and various methods of synthesis. Following which, a specific class of polymers are discussed, influencing the choice of polymer for this work.

2.1. POLYMERS AND GOVERNING TERMINOLOGIES

A polymer can be defined as a substance that is made up of macromolecules (comprised of monomers, contributing to the structure) and can form branches between two or more constitutional units through a number of physical or chemical mechanisms [27]. Polymers can be broadly classified based on their structure, molecular forces and their origin [28] as seen in figure 2.1.

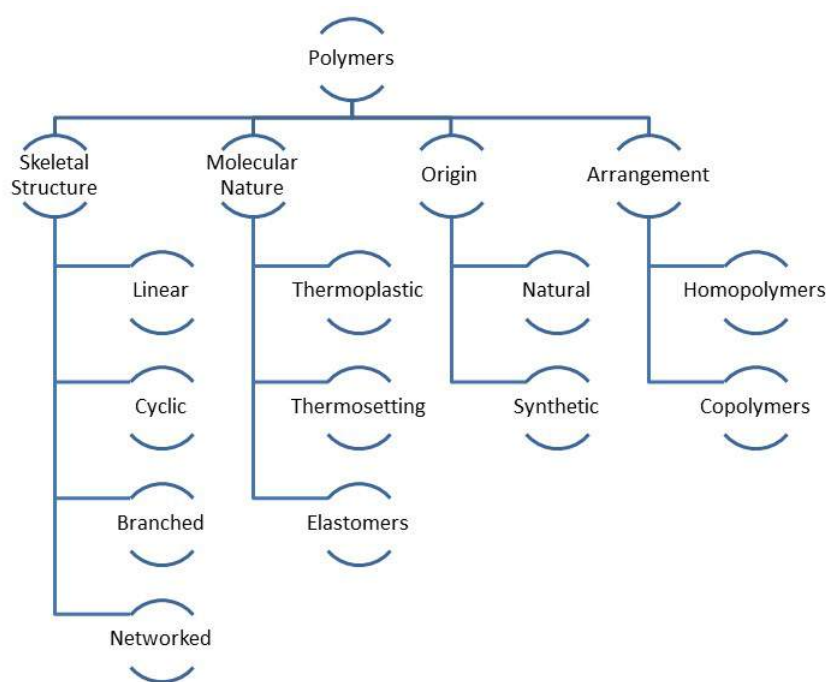


Figure 2.1: Classification of different types of polymers

It is important to note the difference within certain sub-classes from those mentioned in figure 2.1. Primarily, the differences between linear, branched and networked polymers as well as between homopolymers and copolymers [28]. A single chain of monomers that have two definite ends are **linear** in nature and when these chains have side chains linked to them at certain nodes or junctions they are identified as **branched polymers** [28]. A multiple number of such chains when connected to each other, gives rise to a three-dimensional structure resulting in the formation of a **networked polymer** [28].

Similarly, a **homopolymer** consists of many identical monomer units connected to each other, whereas a **copolymer** is made up of more than one type of monomer unit [28]. While the classification will not be discussed in more detail, it is however, still useful to note additional terminologies related to this work that originate directly or indirectly from the classification itself.

Linear copolymers having repeating units that are (in blocks) of the same type, which are usually present as a long sequence [28] are known as **block copolymers**. IUPAC describes a polymer comprised of molecules that have ionizable groups and/or ions, as a **polyelectrolyte**. When a sizable number of such units of a polymer have negatively charged ions and a equal amount of counter-cations then it is an **anionic polymer**, and if vice-verse then it is a **cationic polymer**. Similarly, if both cations and anions are present in a single polymer then it is **ampholytic or neutral polymer** [27].

When polymers are formed by living organisms (biomacromolecules) they are known as a **biopolymers** [29]. However, a **biocompatible** substance is one that has the capability to be in harmony with a living system without producing an unfavourable or harmful effect [29]. Whereas, **biodegradable** refers to the phenomenon of degradation due to biological activity [29].

This particular research project demands the use of biocompatible polymers or other chemicals at every step of the experimental protocol to be food grade and/or biodegradable in nature, for human consumption. Furthermore, it is important to note the phenomenon by which these individual polymer chains form three dimensional networks. The potential of such a class of materials provide great use in a number of domains, especially in biomedical, food and pharmaceutical applications [30].

2.2. HYDROGELS

Before delving into the details of another class of materials such as hydrogels, it is important to understand what they are and how they are formed.

An amalgamation of polydisperse (macromolecules of varying molar masses) branched polymers that are soluble are referred to as a **sol** [31]. As the size of these branched polymers increase a **gel** is formed, which is a non-fluid polymer network that is expanded throughout its entire volume by a fluid formed through physical or chemical bonds [27, 31]. This conversion from a fixed number of branched polymers to an infinitely large molecule is referred to as **gelation**. And a gel wherein the swelling agent is water gives rise to a hydrogel [27].

Hydrogels are a class of polymers that possess a networked structure obtained via cross-linking of their polymeric chains, allowing them to trap considerable amounts of water. These cross-links aid in retaining their swelling behavior in an aqueous environment and prevent the hydrophilic polymer chain groups from dissolving [32], hence, they find various biomedical applications [30] in drug delivery and tissue engineering among many others [33]. They can be classified based on a number of categories [34] as shown below in figure 2.2.

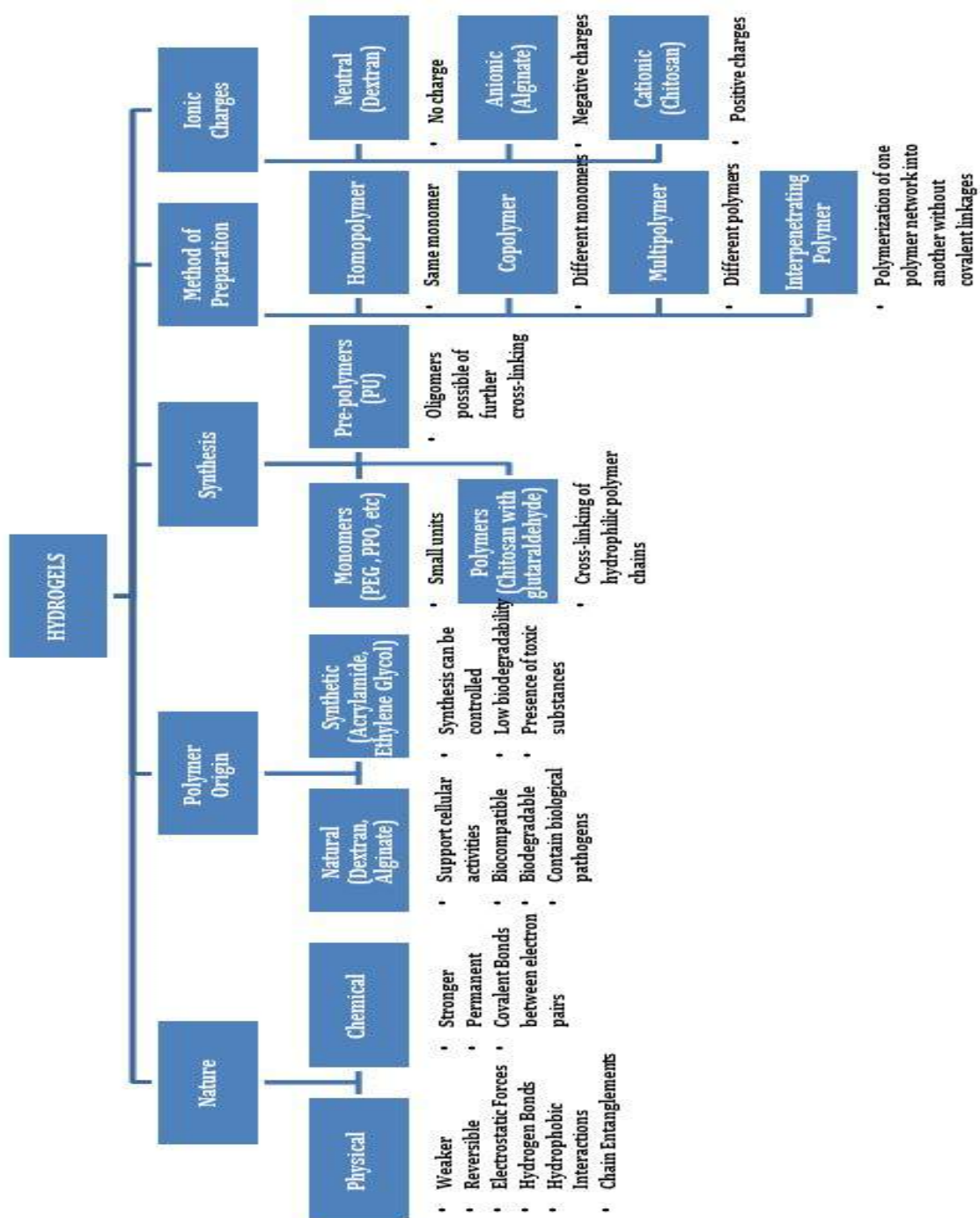


Figure 2.2: Classification of Hydrogels

Although the classification as seen in figure 2.2 is extensive and gives a broad understanding of the characteristic properties specific to each class of hydrogels, for the purpose of this research work, only a particular class will be studied. Specifically, naturally available polymers that are ionic in nature and cross-linked physically to form a hydrogel, are of more importance than others, as will be further discussed in section 2.4.

Hydrogels are also attractive because of the following benefits, however, the limitations that they possess play a prominent role in the appropriate selection for a particular system or application :

Table 2.1: Advantages and limitations of hydrogels in general [34]

Benefits	Limitations
Good Biocompatibility	Poor mechanical strength
Biodegradable; bioabsorbable	Difficult to handle
Good transport properties	Sterilization is not easy
Admissible <i>in vivo</i> through injections in a liquid state	Possess non-adherent properties ¹
Timed release of medicines/nutrients	Higher cost

Hydrogels being made up of over 90% water, possess hydrophilic surfaces which have low interfacial free energy. Therefore, proteins and cells containing hydrophobic moieties have poor affinity towards the surface. Hence, the intermediate compounds formed can be converted into harmless products or made to exit the body without any harm [32].

These properties possessed by hydrogels are of utmost importance and influence the selection of the polymer and method of cross-linking for this project. There are various mechanisms by which cross-linking can be advocated, as discussed in the next section.

2.3. CROSS-LINKING OF HYDROGELS

A cross-link can be defined as a section or region in a macromolecule from which a minimum of four chains arise due to reactions between sites or groups on the existing macromolecule [27].

Apart from the molecular weight and the chemical composition of the polymer that is under consideration, the physicochemical properties of a hydrogel is governed by the method and density of cross-linking [30]. There are various methods by which the labile bonds that are required [32] are introduced in biocompatible polymers through cross-linking, broadly classified into two types [35] as discussed in the upcoming sub-sections.

2.3.1. CHEMICALLY CROSS-LINKED GEL

Chemically cross-linked gels are obtained when the polymer network is formed through covalent cross-links, i.e., basically when a stronger bond takes the place of hydrogen bonds resulting in a rather permanently networked gel [31]. This type of covalent bonding can be synthesized through various mechanisms such as radical polymerization, chemical reaction of functional groups, high energy irradiation and by using enzymes [32].

As mentioned earlier, this method is employed when the mechanical strength of the resulting hydrogel is of utmost importance [35]. The permanent network, apart from providing good mechanical strength also enables free diffusion of water which is an important factor when applied in drug delivery systems and in cell-culture as scaffolds [36]. However this method requires the addition of a cross-linker which could be potentially toxic and undesirable [32] as well as increases the number of chemicals required, which, based on the application, need not always be beneficial.

¹They can be inherently safer to use in the food and pharmaceutical industries if care is taken and applicability is specific.

2.3.2. PHYSICALLY CROSS-LINKED GEL

Gels which are cross-linked through reversible mechanisms like molecular entanglements and/or ionic forces, hydrogen bonding or hydrophobic interactions [31] are known as physical gels. This is a method employed when there is a need to overcome the above stated problem of undesirable toxicity, as it does not require the addition of any cross-linkers for the formation of hydrogels [35].

The interest in this type of cross-linking is also picking up rapidly because it is a mechanism that can be advocated without a purification and verification process [36]. Moreover, it is devoid of the use of organic solvents and can be employed under mild conditions making it very useful in biological and biomedical applications [32]. Based on the type of polymer used, there are various techniques of physical cross-linking that can be employed. Ionic cross-linking is one such method that attracts the focus of this research.

IONIC INTERACTION BASED CROSS-LINKING

Ionic polymers which are cross-linked by the addition of bivalent or trivalent counter-ions [31] fall under this classification. This underlying principle is useful for the gelation of poly-electrolytic solutions with ions of the opposite charge [31]. A popularly known polymer that is most often cross-linked via ionic interactions is Sodium Alginate (Na-Alg), using bivalent ions, most commonly calcium ions [32]. In this project, this method of cross-linking is most suitable for three major reasons:

- In line with the scope of the applicability of this research project, it is important that the chemistry involved in each step of the experimental procedure can be defined which becomes slightly more difficult when the method of chemical cross-linking is adopted.
- The addition of toxic cross-linkers can be avoided and this is an important factor in the focus of this research project as discussed in section 2.3.2.
- Most importantly, the focus of this project is to have an edible end product, therefore, the choice and use of chemicals must be undertaken attentively, therefore all the materials that we utilize must fall under the GRAS chemical category. Na-Alg falls under this category, further influencing the polymer choice and method of cross-linking chosen for this work.

2.3.3. GENERALLY REGARDED AS SAFE (GRAS) POLYMERS

The Food and Drug Administration (FDA) defines a GRAS substance as any substance or a chemical that is deliberately added to food, is subjected to review and approval, unless it is considered safe based on expert advice through scientific procedures or one that has been used in food prior to 1958 and is exempted from the Federal Food, Drug, and Cosmetic Act (FFDCA) food tolerance requirements [37].

As discussed earlier, one such GRAS polymer that is of particular interest with regard to this project is Na-Alg which will be considered in detail in the next section.

2.4. SODIUM ALGinate

2.4.1. INTRODUCTION

Alginate is a naturally available anionic polysaccharide and is commonly derived from brown algae, *Phaeophyceae* such as *Laminaria hyperborea* [30] and *Lessonia* [38]. Alginic

acid is converted into Na-Alg upon processing with aqueous alkali solutions such as NaOH followed by filtration with NaCl to expedite it in its powdered form [39].

2.4.2. STRUCTURE

Structurally, it is a linear, unbranched block copolymer with identical monomer units of (1,4)-linked β -D-mannuronic acid (M) wherein the glycosidic bonds are equatorial and α -L-guluronic acid (G) [38] have axial bonds as seen in figure 2.3. Such G and M residues are connected via covalent bonds arranged in successive G blocks (GGGGGG), successive M blocks (MMMMMM) and alternating G and M blocks (GMGMGM) [30].

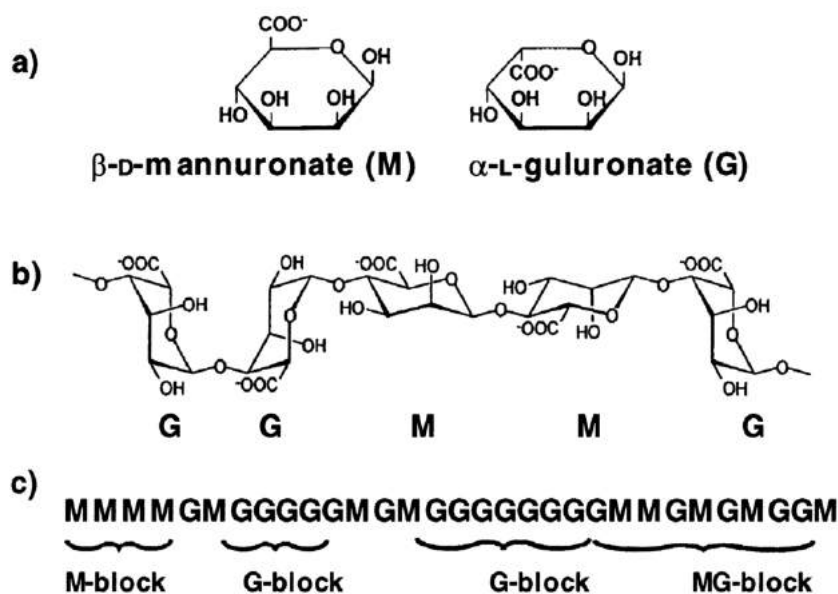


Figure 2.3: Structure of Alginate: (a) alginate monomers; (b) chain conformation; (c) distribution and arrangement of the blocks [40]

The starting material from which Na-Alg is obtained plays a role in defining the ratio of G and M residues as well as the extent of each block [30]. It is also known that the G-blocks of alginate are solely responsible for the conversion of the polymer into a hydrogel via inter-molecular cross-linking [30] between the carboxylic groups and divalent cations [38]. Several properties contribute to the physical properties of alginate and its respective hydrogel [30] as mentioned below:

- Content of M/G blocks and their arrangement with respect to one another
- The length of the G-blocks as it contributes to the mechanical properties of Na-Alg. Furthermore, the G blocks are solely responsible for the intermolecular cross-linking to form hydrogels
- Molecular weight of the alginate which depends on the source from which the alginate is extracted

Furthermore, these physical properties have an influence on the stability and stiffness of the resulting gel-network. It was concluded by Draget *et al.* that alginate contains four feasible patterns (relating it to the flexibility of the chain blocks) of glycosidic links : equatorial (MM), axial (GG), equatorial-axial (MG) and axial-equatorial (GM) [40].

Any alteration in the ionic strength of an alginate solution will have a great effect on the length of the polymer chain and the viscosity of the gel formed. As this ionic strength increases, it will have an influence on the solubility as well [40]. It is also important to note that alginate can be cross-linked at room temperature and physiological pH, making it a more desirable polymer choice for the purpose of cross-linking [32].

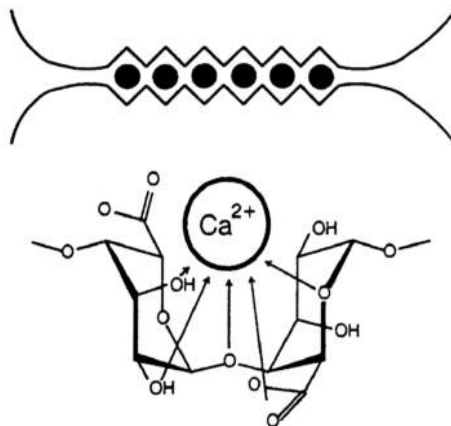


Figure 2.4: Egg-box structure representing the cross-linking mechanism of the G blocks of Na-Alg into calcium alginate hydrogel [40]

Figure 2.4 is a pictorial representation of the G blocks of Na-Alg cross-linking with the Ca^{2+} ions. Upon binding to the G blocks of individual polymer chains, the blocks then tend to join together with the G blocks adjacent to another polymer chain leading to an “egg-box” shaped structure [30]. This defines the mechanism by which the Na-Alg polymer chains undergo gelation to form calcium alginate hydrogels.

2.4.3. ADVANTAGES AND USES

It is abundant availability in a natural environment, biocompatibility, relatively low cost compared to other biocompatible polymers and low toxicity are the factors that contribute towards making Alginate an attractive polymer [30]. Furthermore, from an industrial standpoint, Alginate is favorable due to its hydrophilic, viscous, stabilizing, mildly reversible gelation properties and that the sol/gel transformation is not specifically governed by temperature [40].

It has vast applications in wound healing, drug delivery [40], as an emulsifier/stabilizer in the food sector [38] as well as bio-medical and pharmaceutical applications [30] as discussed in section 1.

2.5. THESIS OBJECTIVES

The research presented here is inspired by the work published by Eral and his collaborators on biodegradable microparticles for detecting authenticity of medicines [1]. While the objective of this thesis is based on the same ideology and concept, the underlying methods are however, different.

The work presented in this thesis is twofold. The research includes experimental implementation of a proof of concept to study and develop edible barcodes² from ALG and the structural behaviour of these barcodes on drying. This work is conducted keeping in mind the end application of this concept, i.e., to detect counterfeit consumables and improper storage of mainly food and pharmaceutical products. Therefore, the goals of this thesis were as follows:

- Developing research strategies and experimental protocols to create ALG barcodes.
- Optimization of the experimental protocol to further enhance the macroscopic structure of the barcodes.
- Study of the influence of drying on the macroscopic structure of these developed barcodes.

² For future reference in this thesis, the term “barcode” refers to the “TU” on the ALG samples

MATERIALS AND METHODS

In this chapter the materials used and the protocols that were followed while conducting the experiments are discussed. These experiments were performed in order to introduce a proof of principle based on the concept presented in the preceding section.

3.1. MATERIALS

An overview of all the materials used are presented in table 3.1. All the chemicals were used as is without further processing. The water used during this entire thesis is deionized water from an in-house dispenser at room temperature and atmospheric pressure.

Table 3.1: Overview of chemicals utilized

Chemical	CAS#	Abbreviation	Purity	Supplier
Sodium Alginate	9005-38-3	Na-Alg	Food grade	Sigma Aldrich
Sodium Chloride	7647-14-5	NaCl	≥99.5%	Sigma Aldrich
Calcium Carbonate	471-34-1	CaCO ₃	Analytical grade	MERCK
Glucono- δ -lactone	90-80-2	GDL	≥99.0%	Sigma Aldrich
Calcium Chloride	10043-52-4	CaCl ₂	≥93.0%	Sigma Aldrich
HEPES	7365-45-9	HEPES	≥99.5%	Sigma Aldrich
Indigo Carmine	860-22-0	-	Bact.,Hist.	Sigma Aldrich

3.2. SYNTHESIS OF ALGINATE HYDROGELS

In the following sub-sections, the preparation of Na-Alg polymer solutions will be discussed. Afterwards, a detailed description of the experimental protocols used to make the ALG hydrogel barcodes² will be presented. It involves a two-step curing process based on the mechanism of ionic cross-linking as described in sub-section 2.3.2.

3.2.1. PREPARATION OF NA-ALG SOLUTIONS

To make aqueous solutions of Na-Alg, first a solution of 0.3 M NaCl and 20 mM HEPES (optional) were mixed with DI water [41]. To this solution, Na-Alg powder was added and stirred on a hot plate at 46°C using a magnetic stirrer at 400 rpm for approximately 45 minutes and/or until all the Na-Alg was dissolved. The required Na-Alg was added accordingly to obtain different, final Na-Alg concentrations of 2, 4, 6, 8, 10 and 12% w/w respectively [41].

3.2.2. FIRST PHASE OF CURING

Once the above Na-Alg solution was homogeneously mixed, CaCO₃ and GDL were added to the mixture while stirring to achieve a final concentration of 20 mM of CaCO₃ while

²The term “barcode” refers to the “TU” on the ALG barcode

maintaining the ratio of $[GDL]/[Ca^{2+}] = 2$ [41]. To facilitate this, an inert form of $[Ca^{2+}]$ ions for cross-linking is obtained from $CaCO_3$ as the source. The solubility of $CaCO_3$ is low in pure water, this allows for it to be evenly distributed in the Na-Alg solution prior to the start of the gelation process [2]. The GDL aids in slow hydrolysis of the solution (by bringing down the pH and enhancing the release of Ca^{2+} ions) [41] so as to obtain a more ordered structure of the hydrogel [2]. This mixture was stirred until a homogeneous ALG hydrogel mixture was obtained. This solution was then centrifuged to remove any air bubbles trapped within the hydrogel and cured in the refrigerator (at $4^\circ C$) for 24 hours. Air bubbles need to be removed in order to obtain clear measurements for further analysis of the samples, particularly for the higher Na-Alg concentrations used [41] and to maintain a uniform structure of the hydrogel.

3.2.3. SECOND PHASE OF CURING

For further cross-linking of the hydrogel, a 6% w/w aqueous solution of $CaCl_2$ in DI water was prepared [41]. 3 ml of this solution was mixed with the previously-made hydrogel and was allowed to cure again for an additional 24 hours at approximately $4^\circ C$ in the refrigerator [41].

If the hydrogel sample was not cured homogeneously (or completely, due to less coverage of $CaCl_2$ over the entire sample) then it was allowed to cure, undisturbed for another 24 hours. The homogeneity of the hydrogel was ensured based on the coverage attained by the $CaCl_2$ solution through the hydrogel mixture and its initial quantity used for cross-linking. Greater curing time ensures better permeation of $[Ca^{2+}]$ ions to all the available binding sites for cross-linking [41]. Once the hydrogel was completely cured, it was manually cut into cylindrical discs or cuboids of varying dimensions based on the mould used for curing the hydrogel and/or based on the desired requirement for post processing. A schematic of the experimental setup describing each step of the procedure followed can be seen in figure 3.1.

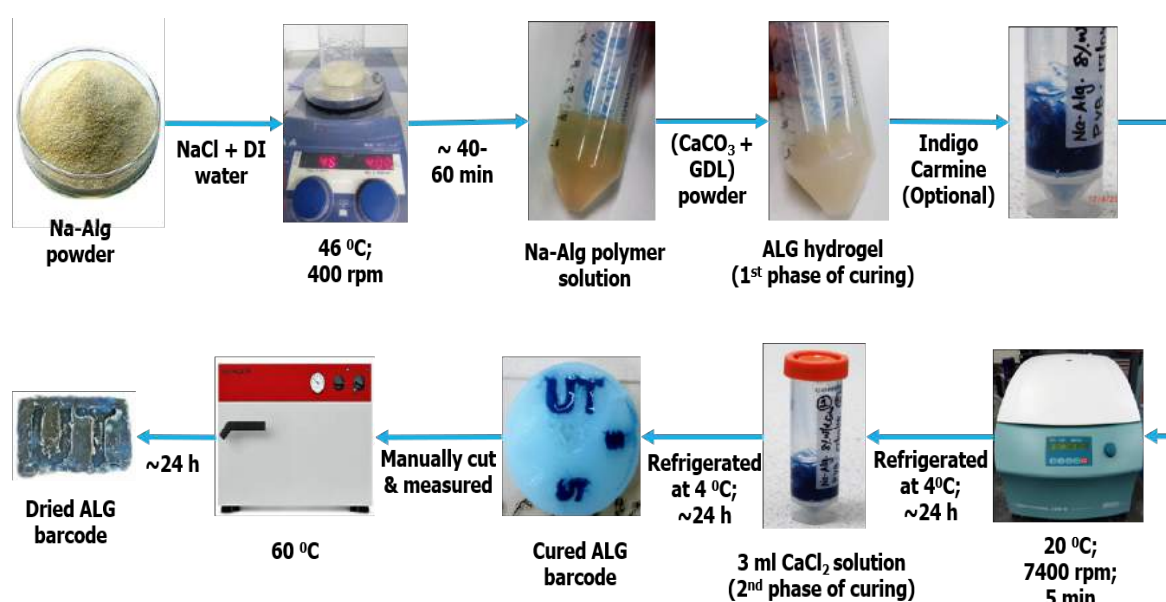


Figure 3.1: Schematic of experimental setup used to make the ALG barcodes

3.3. MOULDS FOR CURING OF HYDROGEL

3.3.1. METAL STAMPER

The 3D printed metal stampers which were fabricated from a study (refer [42]) done previously in the group were used as a mould for the first trial to cure the hydrogel. Two different stampers of different sizes and shapes were used as a mould for the same. Due to the material properties of the stamper (made of sintered steel and aluminium), the hydrogel was poured into the mould after the first phase of curing, as described in section 3.2.2 (before addition of CaCl_2) and left in the refrigerator for 24 hours (at 4°C) to prevent corrosion of the stamper.

The hydrogel in the mould was then pressed out of the stamper manually. Care was taken so as to not distort the structure of the hydrogel since it had not undergone the second phase of curing yet. It was taken through the remaining steps for further curing as described previously in subsection 3.2.3.

The metal stamper, although a good starting point was not the best option for cross-linking as the barcode-laden hydrogel could not be reproduced successfully with the same or at the least, a similar output each time. Also, it yielded a successful output only for one particular Na-Alg (6% w/w) concentration of the hydrogel as observed from conducted experiments.

In order to account for the shortcomings of the barcodes made from the metal stampers, it was decided to develop another mould with different material properties for curing the ALG hydrogel.

3.3.2. 3D PRINTED POLYMER MOULD

A 3D printed polymer mould was designed using a 3D CAD software - Inventor[®] and fabricated from ABS flex white with the barcode "TU" printed from a Micro Plus HD 3D printer by EnvisionTEC[®] (refer figure 3.2). Three different dimensions of the barcode (10 x 6 mm, 5 x 3 mm and 3.5 x 2 mm) all with 1 mm thickness (of the "TU") were printed (extruded) on the flat surface of the same mould. The idea behind this design was to aim at circumventing the problems that were associated while working with the metal stampers as discussed in section 3.3.1.

Specifically, the justification for this was twofold, namely:

- To ensure that the mould could be used for all the above studied concentrations of Na-Alg (i.e., 2, 4, 6, 8, 10 and 12 % w/w).
- To optimize the curing process in the mould in an attempt towards increasing its efficiency, convenience and simplicity of the process.

This was done by making a design of the mould in such a way that the hydrogel could be cured immediately after the centrifuging step, i.e., the mould was fitted into a 50 ml Corning[®]falcon tube and the hydrogel (after the first phase of curing) was poured into the falcon tube over the mould (refer figure 3.2). It was then centrifuged at 7400 rpm for 5 minutes and refrigerated for 24 hours.

Figure 3.2 indicates the design of the 3D polymer mould fitted into the falcon tube. Another advantage of using this mould over the metal stamper was that the complete curing phase over the time period of approximately 48 hours was carried out without disturbing the structure of the hydrogel or further incorporating air bubbles into the hydrogel matrix.

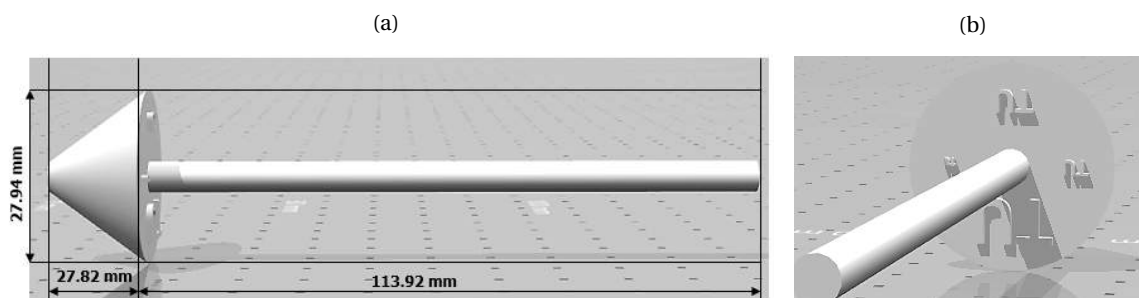


Figure 3.2: 3D printed ABS flex white polymer mould designed using Inventor[®] and printed from EnvisionTEC[®] 3D printer. (a) Lateral view of the mould (with the “cone” end connected to the “stem”). (b) Top view of the mould with “TU” barcode

3.4. POST PROCESSING

Once the hydrogels were completely cured, they were manually cut around the barcode for further studies on the maintenance of their structure and loss of mass as a function of time. For this purpose, the hydrogel samples were oven dried to observe the deformation of the barcode structure and decrease in thickness and size. Thermogravimetric studies were also conducted to analyze the mass loss as a function of time for the ALG hydrogel samples.

3.4.1. DRYING

The cut out hydrogel barcodes were pat-dried gently on a tissue paper to remove the excess water and curing solution. After which the mass and dimensions of each of the samples were recorded. The samples were then oven dried at 60°C. The same measurements were recorded again after set, regular intervals of time. This was repeated until it was observed that there was no further change in the dimensions or loss of mass of the samples.

The change in the structure of the sample, especially the distortion of the “TU” barcode and the dimensions, especially thickness of each sample was of utmost importance during this drying process. As discussed before, since the results obtained from the experimental protocol were not as promising as required, optimization of the protocol was imperative, as considered in the next subsection and in detail in section 4.2.

3.4.2. ALTERATIONS IN THE PROTOCOL

After studying the structure of the hydrogels post drying, it was necessary to understand other contributing factors affecting the macroscopic structure of the ALG barcodes, as discussed in section 4.3. It was decided that the deformations in the structure could be reduced if the hydrogels were made more robust. Therefore, in order to verify if the concentration of the components responsible for cross-linking had an effect on the durability of the barcodes, further experiments with alterations in the experimental protocol were conducted to validate this claim.

For this purpose, the $[\text{GDL}]/[\text{Ca}^{2+}]$ concentration ratio was kept constant, however, the mass of CaCO_3 and GDL added were doubled, whereas that of other chemicals used were unaltered. Therefore, the same experimental protocol was followed in the same order of steps, the only difference being the change in concentration of CaCO_3 and GDL added to the hydrogel mixture in the second phase of curing (refer 3.2.3)

It was expected that increasing the concentration of CaCO_3 would thereby increase the Ca^{2+} ions available for cross-linking. However, it is important to note that this would also lead to an increase in the total percentage of the involatile components with respect to the increase in Na-Alg concentration.

The structure of the barcodes, especially in terms of thickness and size, post drying was a relevant factor for this project and an experimental protocol that would facilitate that with the best outcome was necessary. An explanation of the results obtained from the experiments described in this chapter will be discussed in detail in the upcoming chapter of this thesis.

4

RESULTS AND DISCUSSION

This chapter focuses on the results associated with the development of the hydrogel barcode² as a proof of concept made from different concentrations of Na-Alg using two moulds of different material properties. Furthermore, the structural deformations of the barcode on drying and thermogravimetric analysis was studied. Finally, the effect of change in concentration of the components responsible for cross-linking of Na-Alg on the barcodes will be considered.

4.1. MOULDS FOR CURING OF HYDROGEL

For the ALG hydrogel to take the shape of the barcode on itself, different 3D printed moulds made from different materials - metal (rectangular and circular moulds) and polymer (ABS flex white) were used. They were fabricated with the extrusion of a “TU” shape as a prototype for the barcode. The results and observations for the same will be discussed in the upcoming sections.

4.1.1. METAL STAMPERS

The experimental procedure with two-phase curing was followed to develop the hydrogel barcode for all concentrations of Na-Alg (ranging between 2% w/w and 12% w/w), as mentioned earlier in section 3.2.1. Two types of 3D printed metal stampers (rectangular and circular shaped), previously available in the lab, were used as a mould to cure the hydrogel as seen in figure 4.1.



Figure 4.1: Metal stampers available that were used to cure the Na-Alg, fabricated and designed from previous work [42]. Scale bar: 2.7 mm

It is important to note that the two metal stampers are made of different materials [42]. The rectangular metal stamper is 3D printed from sintered alloy of steel while the circular

²The term “barcode” refers to the “TU” on the ALG hydrogel samples

metal stamper is fabricated from aluminium. The following observations were made about the effectiveness of these moulds on curing the hydrogel:

- **Rectangular metal stamper:**

The hydrogel cross-linked satisfactorily with the “TU” barcode imprinted on it in the rectangular shaped metal stamper as seen in figure 4.2. Figure 4.2a shows the method in which the hydrogel is allowed to cure in the metal stamper.

The clarity of the “TU”, imprinted as the barcode, although poor was visible to the naked eye, as seen in figure 4.2b. However, this was observed only with the 6% w/w Na-Alg concentration. The lower or higher than 6% w/w Na-Alg concentrations used in this study could not cross-link (cure) well enough to maintain their structure in the rectangular metal stamper (refer table 4.1).

However, a qualitative reason why the 6% w/w Na-Alg was the only concentration able to cure in the rectangular stamper could be ascribed to the concentration of Na-Alg and $[GDL]/[Ca^{2+}]$ that make-up the ALG from 6% w/w Na-Alg . It could be suggested that this particular concentration was optimum to allow for it to cure in the rectangular metal stamper.

It could be also be assumed that the concentration of Ca^{2+} ions was sufficient to occupy all the binding sites available to cross-link the Na-Alg completely during the 1st phase of curing. Thus, preventing the inhibition of the curing process (due to any other side reactions) as this was not observed with the other concentrations of ALG hydrogels.

However, additional tests were not conducted to verify the claim stated above (as to what caused the hydrogels to not cure in the metal mould) as it was not within the scope of this research work.

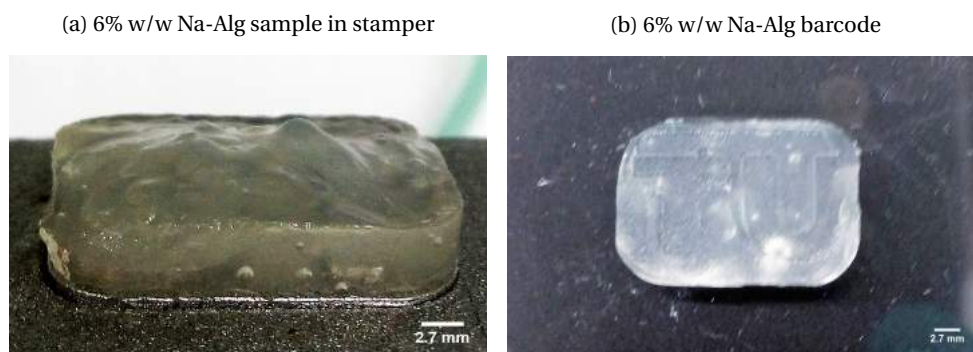


Figure 4.2: 6% w/w Na-Alg sample cured in the rectangular metal stamper (after 24 h of 1st phase of curing). (a) Sample of 6% w/w Na-Alg allowed to cure in metal stamper (b) Cured sample of 6% w/w Na-Alg when removed out of the metal stamper with “TU” imprinted on the ALG (before 2nd phase of curing).

- **Circular metal stamper:**

The hydrogel samples of different concentrations were now also allowed to cure in the circular shaped metal stamper previously available in the lab. As the 6% w/w Na-Alg cured in the rectangular stamper, it was necessary to further examine if the barcode could be sized down. Sizing down of the barcode was an important criterion with respect to the end applicability of this concept. Therefore, apart from having a

different geometry, the dimensions of the “TU” barcode were smaller on the circular metal stamper (10 mm diameter), making it useful to validate if the hydrogel barcode could be scaled down.

However, it was observed that none of the samples including 6% w/w Na-Alg, or the other concentrations of Na-Alg used earlier, were able to cure and maintain their structure in this metal stamper as seen in figure 4.3. Figure 4.3a shows the method by which the hydrogel sample was cured in the stamper. It was seen that the hydrogel was not able to maintain its structure and cure well in this stamper as seen in figure 4.3a. The difference in the structure of the hydrogel is distinct as was seen with the rectangular stamper in figure 4.2a.

In essence, transferring the imprint of the circular stamper onto the hydrogel sample as a barcode (refer figure 4.3b) was not successful for any concentration of Na-Alg considered (also refer table 4.1).

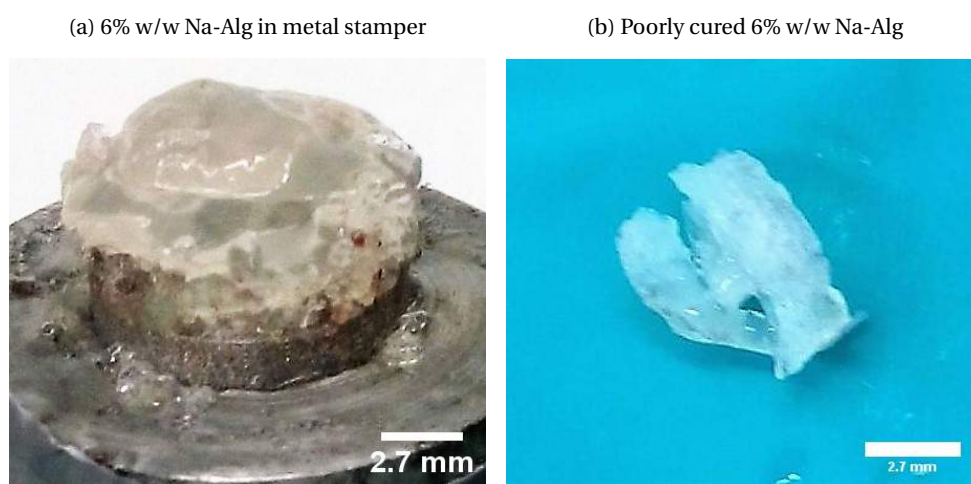


Figure 4.3: 6% w/w Na-Alg sample in circular metal stamper (after 24 h of 1st phase of curing). (a) Sample of 6% w/w Na-Alg allowed to cure in metal stamper (b) Poorly cured sample of 6% w/w Na-Alg when removed out of the metal stamper (before 2nd phase of curing).

The experiment was also carried out with the addition of HEPES (pH range 6.8-8.2), used as a buffer to maintain the physiological pH of the system [43] and therefore, to improve the longevity of the prepared sample. The following results were observed:

- **Rectangular shaped metal stamper:**

The Na-Alg did not cure (cross-link) for the 6% w/w Na-Alg concentration when HEPES was added, unlike observed earlier when cured without the addition of HEPES (refer figure 4.2). It did not cure for the other concentrations of Na-Alg used in this study either.

- **Circular shaped metal stamper:**

The Na-Alg failed to cure and take the print of the “TU” barcode on itself with this stamper for any concentration of Na-Alg used in this work.

Furthermore, on allowing the hydrogel to cure in the circular stamper for approximately 10 days, it was seen that the two independent parts of the stamper were fused tightly together and could not be separated even after cleaning several times, as seen in figure 4.4.

It is speculated that this could be due to the deposits (of the components used to make the hydrogel sample) settled on the stamper and their reaction with the material (aluminium) of the metal stamper.



Figure 4.4: Reaction of 12% w/w Na-Alg (with HEPES) in the circular stamper after allowing the hydrogel to cure for \approx 10 days

Following the results obtained from the experiments above, some inferences can be drawn as to why the hydrogel samples could be cured exclusively with the rectangular metal stamper and only with the 6% w/w Na-Alg concentration, without the addition of HEPES:

- As the two metal stampers used were made of different materials, it could be speculated that this was one of the reasons for the hydrogel to cure only in the rectangular stamper (made from sintered steel alloy).
- To summarize, the assumption for the hydrogel not curing in the metal stampers can be associated to the reaction of one or more of the components present in the hydrogel (the insolubles) with the material properties of the stamper. Further experiments were conducted on the circular metal stamper in an attempt to validate this claim. It was subjected to testing by allowing it to stand for 24 hours separately in solutions of the individual components, in the same concentrations as used to make the hydrogels (refer section 3.2). This was done to verify which of the chemical components affected the metal most.

The results indicated that the circular metal stamper was most affected when placed in a 20 mM aqueous solution of CaCO_3 and DI water, in comparison to NaCl, Na-Alg, GDL and HEPES (refer appendix C). Therefore, we can suspect that this could be one of the major contributing factors for the failure of curing of the hydrogel in the circular metal stamper.

In order to circumvent the challenges and limitations faced with the use of the metal stampers, another 3D printed mould was fabricated from ABS flex white polymer as an alternative. The results obtained from the experiments are discussed below.

4.1.2. 3D PRINTED POLYMER MOULD

The experiment was conducted for all concentrations of Na-Alg (refer table 4.1) as mentioned earlier in section 3.2.1, similar to that done with the metal stampers. The following observations and discussions could be noted:

- The improved mould with regard to the design and material, effectively aided in curing all the concentrations of Na-Alg considered in this study. The results obtained were successful each time the experiment was conducted in terms of a “TU” embossed barcode when compared with those obtained from forging the hydrogel with the metal stampers, as discussed in section 4.1.1.

The experimental protocol was thus, simplified and optimized as it increased the ease of handling by reducing a couple of intermediate steps of the protocol. Namely, manual transfer of the hydrogel samples from one container into another after each phase of curing was avoided with the new mould. This in turn minimized the non-uniformity of the structure of the hydrogel due to breaking, as well as incorporation of air bubbles into the hydrogel matrix post centrifuging.

Apart from overcoming the challenge of uncured hydrogel barcodes, a prominent criteria in this work, it also resulted in the vast improvement of the visibility of the “TU” barcode on the hydrogel for each of the concentrations of Na-Alg, with or without the addition of HEPES, as seen in figure 4.5. Figure 4.5 shows the “TU” imprinted barcodes following the same experimental protocol, as discussed in section 3.2. Three different sizes of the “TU” barcode on the same sample can be seen in all the figures. The clarity of some of the samples (refer figure 4.5e and figure 4.5f) were not as expected due to incorrect manual handling while removing the sample from the mould and can be avoided by gentle handling of the hydrogel samples through practice.

- It can also be concluded that in principle, the hydrogel samples could now be centrifuged, stored and both phases of curing could be undertaken in the same mould (in one single falcon tube), without further disturbing the hydrogel matrix before the curing process was completed. In this way, it was ensured that the visibility of the barcode would be enhanced and clear, unlike with the metal stampers.

To summarize, the newly designed ABS flex white polymer based mould was proven that it was a necessary and better choice for this work, when compared with the metal stampers as seen previously. The experimental results demonstrated that the newly designed mould was beneficial as it fulfilled its intended purpose of developing and successfully curing the barcode-laden hydrogel with minimum deformations prior to drying, as seen in figure 4.5.

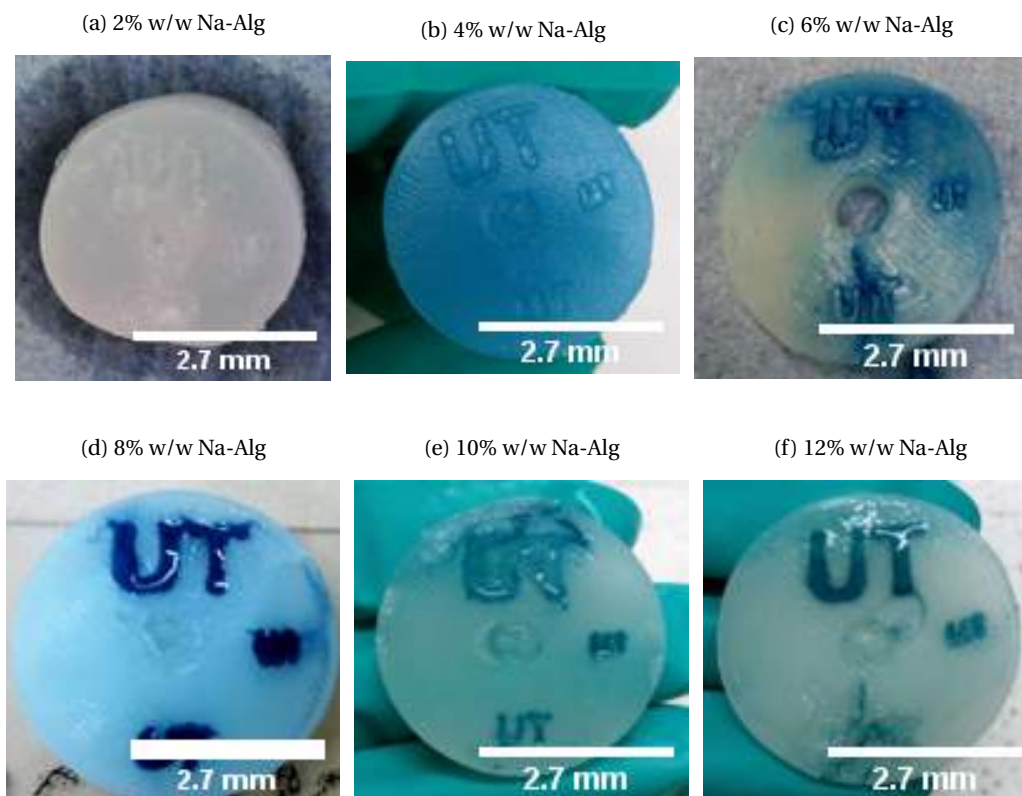


Figure 4.5: From figure (a) to (f): 2%, 4%, 6%, 8%, 10% and 12% w/w concentrations of Na-Alg “TU” barcodes cured using the improved ABS flex white polymer mould. The blue colour of the barcodes is due to the use of indigo carmine dye for the sake of visibility.

Below is a table to consolidate the experimental results with respect to the different moulds that were used for curing the hydrogel barcode. As seen from the table, the polymer mould was most effective (with and without the addition of HEPES) for the system chosen for this work.

Table 4.1: Experimental results for curing of hydrogel in the 3D printed moulds

Na-Alg Concentration	Rectangular Metal Stamper (without HEPES)	Rectangular Metal Stamper (with HEPES)	Circular Metal Stamper (with & without HEPES)	Polymer Mould
12% w/w	×	×	×	✓
10% w/w	×	×	×	✓
8% w/w	×	×	×	✓
6% w/w	✓	×	×	✓
4% w/w	×	×	×	✓
2% w/w	×	×	×	✓

While the barcodes obtained from the above discussed method gave promising results, it was necessary for them to maintain their structure (when manually cut into rectangular shapes enclosing the barcode) post drying in order to realize the requirements for their end application with respect to this work.

4.2. DRYING STUDIES

After the hydrogel had cured uniformly and completely in the mould, it was subjected to drying in an oven at 60°C in order to study the behaviour of these ALG barcodes upon evaporation of water entrapped in them. This step was particularly prominent in this project, as one of the end applications of this proof of concept is for the hydrogel barcodes to be in compatibility with dry food and powdered pharmaceutical products.

An example of the drying process with change in mass and dimensions is seen in figure 4.6 and displayed in table 4.2. The decrease in the dimensions was clearly visible as the drying time progressed. It can also be seen from figure 4.6 that there was a distinct difference in the structure of the barcode post drying.

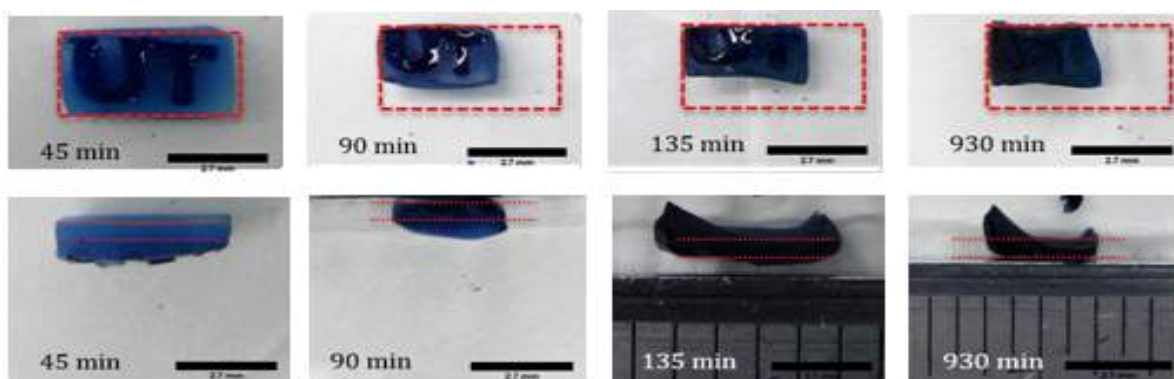


Figure 4.6: Drying of 6% Na-Alg barcodes (20 mM CaCO_3) with change in mass and dimensions over a time period of ≈ 24 h. Scale bar: 2.7 mm

Table 4.2: Change in mass and dimensions over a time period of ≈ 24 h for 6% w/v Na-Alg barcode with $[\text{GDL}]/[\text{Ca}^{2+}] = 2$

Time (min)	Mass (g)	Length (mm)	Width (mm)	Thickness (mm)
0	0.23	12.00	8.00	2.02
45 min	0.15	10.02	7.01	2.00
90 min	0.07	8.00	5.01	1.02
135 min	0.04	7.01	4.02	1.01
930 min	0.03	6.02	4.00	1.00

In an attempt to circumvent the distortions in structures of the barcodes, certain alterations were made to the existing protocol to examine if it led to a decrease in structural deformations of the barcodes as described in section 3.4.2. The results obtained from this experimental procedure are discussed below.

Therefore, two objectives as defined previously in section 2.5 were realized as important at this stage:

- To develop and optimize the design and material of the mould used to make a barcode from ALG hydrogel
- To observe their structural changes on drying the ALG barcodes. Keeping this in mind, it was observed that the barcodes made from the existing experimental protocol had difficulty in maintaining their structural integrity post drying, as seen and discussed in section 4.2.

Therefore, optimization of the experimental protocol was necessary to circumvent or reduce the structural deformations of the barcodes on drying. The results obtained from this study are analysed going further.

4.3. ALTERATIONS IN EXPERIMENTAL PROTOCOL

The experimental results showed that doubling the concentration of the cross-linking agents (GDL and CaCO_3) in the protocol for making the hydrogel barcodes (also refer section 3.4.2) resulted in stronger and more durable structures.

An example of the results obtained from this experiment is shown in figure 4.7 and discussed in detail in sections 4.4 and 4.3.

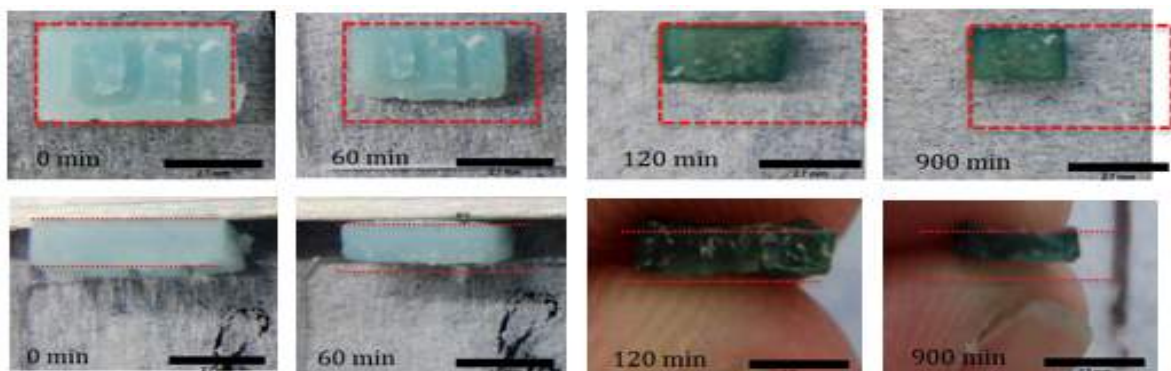


Figure 4.7: Drying of 6% w/w Na-Alg barcodes (with 20 mM CaCO_3 and GDL) with change in mass and dimensions over a time period of ≈ 24 h. Scale bar: 2.7 mm

The dimensions recorded from the figure above for the decrease in mass and dimensions for 6% w/w Na-Alg over a time period of ≈ 24 h of drying (figure 4.7) are tabulated below (table 4.3) for reference and will be discussed further in section 4.4.

Table 4.3: Change in mass and dimensions over a time period of ≈ 24 h for 6% w/w Na-Alg barcode (40 mM CaCO_3)

Time(min)	Mass(g)	Length(mm)	Width(mm)	Thickness(mm)
0	0.16	10.01	7.00	2.01
60 min	0.08	8.01	5.01	2.00
900 min	0.03	5.02	3.02	1.02
960 min	0.03	5.02	3.02	1.02

The alteration in the experimental protocol ensued lesser distortion in the dimensions of the hydrogel samples post drying, considerably, if not entirely as seen in figure 4.7. Thus, it was observed that there was another limiting factor that was contributing to the structure of these hydrogel structures which was independent of the concentration of Na-Alg used.

Furthermore, although the hydrogel samples made from the optimized experimental protocol cured well, increasing the concentration of the cross-linking agents resulted in deposits on the barcodes, especially in the “TU” regions of the barcode as shown in figure 4.8. It was speculated that these deposits could be due to one/many reasons such as, excess calcium crystals or fibres (which might be extruded out of the hydrogel and cured

on the surface on drying), salt crystals (NaCl) that get trapped and settle down after the centrifuging step or a melt from a mixture of unreacted/excess carbonates of calcium and sodium.



Figure 4.8: Deposits on 4% w/w hydrogel barcodes made from optimized experimental protocol. (a) Deposits on barcode before drying. (b) Deposits on barcode after drying. Scale bar: 2.7 mm

It could also be due to the nature of the hydrogel network which might be extruding the unreacted involatiles from their matrix (thereby forming a layer above) that is interrupting the evaporation process of water and hence contributing to a more intact structure post drying. The deposits are speculated to be unreacted CaCO_3 , but can be proved perhaps by performing a SEM with EDX/EDS analysis of the cross-section of a cured ALG sample.

However, it is important to note that the deposits did not inhibit the curing process of the hydrogel as seen previously with the metal stampers (refer section 4.1.1).

The assumption is that a layer of these deposits/involatiles was formed over the barcodes that was interfering with the evaporation of water from the hydrogels. Therefore, resulting in the reduction in deformation and giving rise to more robust structures, as seen post drying, in terms of the dimensions of the barcodes. However, it is recommended to make a note at this point to perform additional compositional analysis (such as XRD studies) to confirm the crystalline structure and nature of these deposits. Analysis of these deposits could also benefit in confirming the above stated hypothesis that the involatiles are contributing significantly to the structural integrity of the hydrogel barcodes.

In conclusion, the deformations of the barcodes of various concentrations of ALG hydrogels were not directly related to the concentration of Na-Alg used. It was expected earlier that higher the concentration of Na-Alg used, the result in-turn would be more robust hydrogel structures. However, since the only change in the experimental protocol made was the increase in concentration of the cross-linking agents, it can be pointed out and hypothesized that the limiting contributors to the structure were the involatiles present in the hydrogel barcodes. Hence, a sensitivity analysis of the aforementioned factors is required to observe the reproducibility of this technique and validate this hypothesis.

4.4. FURTHER DRYING ANALYSIS

The speculation that the buckling of the barcodes is not exclusive to the concentration of Na-Alg requires further reasoning. Although the structures were more durable at higher

Na-Alg concentrations pre-drying, it was however, observed through experiments that the integrity of the structure post drying was not significantly different from each other with respect to barcodes made from higher Na-Alg concentration.

- The experimental results showed that the mass of the hydrogel barcodes reduced rapidly from its initial mass before drying until most of the water trapped within the hydrogel matrix had evaporated, following which the mass of the samples decreased at a slower rate until it reached a constant where further evaporation of water did not take place. This was as expected and beyond this point, the mass and dimensions of the hydrogel barcodes remained constant and drying them further caused no other effects.
- It was expected to find that the loss of water would be minimum for the highest Na-Alg concentration (12% w/w) containing the highest percentage of insolubles and maximum for the lowest concentration of Na-Alg (2% w/w) with the lowest percentage of insolubles, used in this study.

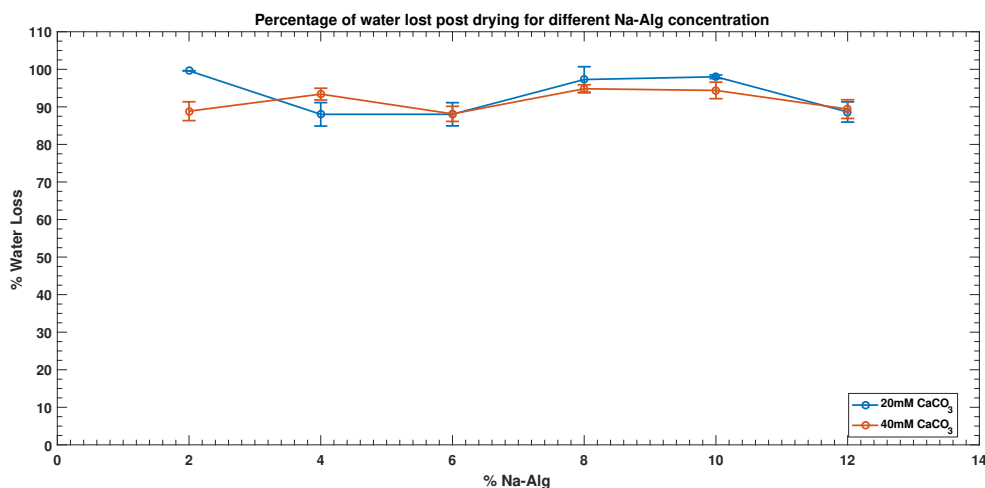


Figure 4.9: Percentage of water lost from the ALG barcodes post drying with respect to the initial amount of water retained before drying, by each concentration of Na-Alg sample considered in this study. The blue line represents the barcode samples made from the initial experimental protocol with 20 mM of CaCO₃ and the orange line represents the barcodes made from the optimized experimental protocol with 40 mM of CaCO₃ (but with a constant ratio of $[GDL]/[Ca^{2+}] = 2$ for both).

However, as seen from figure 4.9 (where the error bars represent the standard deviation arising from repeating the drying experiments in triplicates for samples of each concentration of Na-Alg), this was not what was observed from the experiments. It was seen that the percentage of water lost was independent of the Na-Alg concentration as perceived at the start of this research.

From figure 4.9, it is also observed that the water loss follows the same trend for the samples with an increased amount of cross-linking agents as well. Therefore, indicating that while the percentage of water lost was comparable, there is another governing factor that is contributing to the improvement in the structure of the barcodes with 40 mM of CaCO₃. This further consolidated the earlier claim that the quality of the ALG barcode structure was enhanced with increased concentration of the cross-linking agents, as discussed previously in section 4.3 (also refer section C for the mass balance).

- Furthermore, it was also observed that the method of drying the hydrogel samples played a consequential role in affecting the morphological features of the barcodes. When the samples were dried in a system with constant volume (closed system - covered with a glass lid), it was seen that there was lesser buckling or folding of the edges as compared to when the samples were dried in an open system (without the glass lid).

4.4.1. EFFECT OF VARYING THICKNESS ON THE BARCODES POST DRYING

It is also important to note the structural changes that the barcodes showcased when drying samples of varying thickness.

- The minimum thickness ($\approx 1\text{mm}$) of samples considered in this work, failed to maintain their shape upon contraction, post drying as was required. It was seen that the edges would fold inwards or twist more on the thin edge (right side) of the barcode as the drying time progressed as seen in figure 4.10 below. The values for the decrease in mass and dimensions of the barcode over time can be seen in table 4.4.



Figure 4.10: Drying of (decreased thickness on one end) 8% w/w Na-Alg barcode with change in mass and dimensions over a time period of ≈ 24 h. Scale bar: 2.7 mm

Table 4.4: Change in mass and dimensions over a time period of ≈ 24 h for very thin on one end 8% w/w Na-Alg barcode

Time (min)	Mass (g)	Length (mm)	Width (mm)	Thickness (mm)
0	0.11	11.00	7.00	1.02
45 min	0.05	8.02	5.01	1.01
90 min	0.02	6.01	3.02	1.00
135 min	0.02	6.00	3.02	0.02
930 min	0.01	5.01	3.02	0.02

- However, the same phenomenon was not observed when the samples of maximum thickness ($\approx 4\text{mm}$) considered in this work were dried. It was observed that the ALG barcode samples developed an outer, raised, glassy layer as seen in figure 4.11. The decrease in mass and dimensions of the barcode over time can be seen in table 4.5. It was speculated that a possible explanation for this behavior could be due to buckling instability, as discussed in more detail in appendix A.

To summarize the discussions made earlier in section 4.3, in order to study this behaviour further and gain insight into how to prevent it from occurring, alterations were made to the existing protocol. These alterations led to a more durable ALG barcode structures, wherein it was observed that buckling of the barcodes reduced to a significant extent post drying when compared with the previous samples with increased concentration of

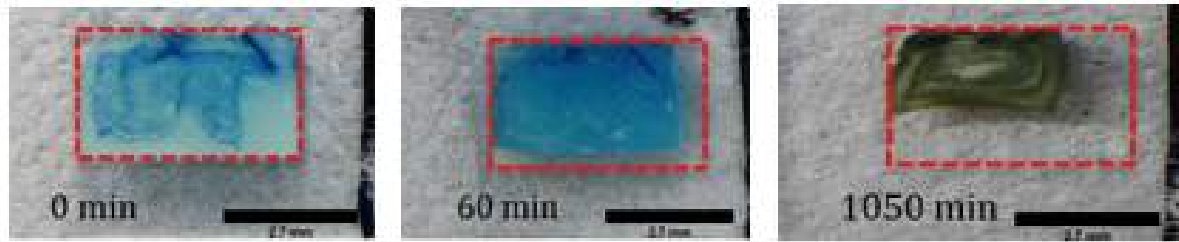


Figure 4.11: Drying of 10% w/w Na-Alg barcode (increased thickness of barcode) with change in mass and dimensions over a time period of ≈ 24 h. Scale bar: 2.7 mm

Table 4.5: Change in mass and dimensions over a time period of ≈ 24 h for very thick 10% w/v Na-Alg barcode

Time (min)	Mass (g)	Length (mm)	Width (mm)	Thickness (mm)
0	0.49	12.01	8.02	4.02
60 min	0.37	11.01	7.02	4.02
1050 min	0.06	7.01	4.02	2.00

the cross-linking agents. However it is recommended for experimentation with further increase in the cross-linking agents (beyond the concentration studied in this work) to truly observe the extent of contribution of the cross-linking agents in maintaining the structure of the barcodes.

As the work presented here is in its initial stages and is qualitative in nature, effort is required to quantify and validate the hypotheses presented in this study. Additionally, it is important to further understand the underlying mechanisms that are involved during/post the drying stage.

5

CONCLUSIONS

The research presented in this thesis is based on concept initiation and provides a qualitative outlook on the development of an edible hydrogel barcode, together with the structural changes influenced by drying. This work discloses promising experimental results that validate the approach towards the end applicability of this concept.

A preliminary prototype for an edible barcode was fabricated from ALG hydrogel using only GRAS chemical substances (refer subsection 2.3.3). The development of a barcode was proved to be possible with the use of the current experimental protocol. Special attention was given to the biocompatibility of the barcode and to ensure utmost simplicity by optimization of the experimental procedure.

With regard to the experimental procedure followed, it was also concluded that the material properties, design and fabrication of the barcode mould are essential and can have an influence on the curing process of the hydrogels. The results indicated that polymer materials (such as ABS polymer) are more suitable (than sintered steel or aluminium) for fabricating the moulds for curing the barcodes.

Furthermore, a remarkable observation in this work was that the concentration of Na-Alg was not the significant contributing factor in maintaining the structural integrity of the ALG barcodes. It was expected at the commencement of this work that higher concentrations of Na-Alg will have more robust structures. This pointed out that there was another limiting factor influencing the structure of these hydrogel barcodes, especially during the drying stage. Further experimental results supported this claim and it was suspected that the involatiles had a consequential involvement in improving the structure of the barcodes. Structure here refers to the macroscopic structure of the ALG barcodes (especially in terms of integrity and stability of the barcodes) post drying. This hypothesis is made based on experimental observations obtained by comparing the structure of the ALG barcodes made from two experimental protocols differing only in the content of CaCO_3 and GDL being added to the hydrogel mixture.

Another contemplation posed was that (not accounting the method of drying applied) the dimensions of the barcode (predominantly the thickness) was a significant factor contributing to the structure of the ALG barcodes. Although further experiments are required to determine the optimum thickness of the barcode, the current experimental results showed that the barcodes maintained their structure better upon drying when cut (roughly) within a certain range of dimensions. That is, when the dimensions were in the the range of $\approx(6-11)$ mm in length, $\approx(4-6)$ mm in width and $\approx(2-3)$ mm thick (for the samples that were cured with the initial experimental protocol with 20 mM of CaCO_3). However, with the optimized experimental protocol (with increased concentration of the cross-linking agents -

40 mM of CaCO_3), it was concluded that the overall structure of the barcode showed good improvement, with reduced deformation in structure post drying.

Furthermore, the experimental results indicated that working with the same range of dimensions as stated above did not have much influence on the structure in comparison to the previous results obtained with 20 mM of CaCO_3 , as long as the thickness of the barcodes are above ≈ 1 mm. This result could also be in agreement with the hypothesis stated above, that the involatiles are one of the governing factors influencing the structure of the ALG barcodes.

Finally, it is also important to note the method by which the hydrogel barcodes were dried. When the barcodes were dried in a closed system, i.e., when the petridish was covered with a glass lid, the structure of the barcodes were observed to have lesser folding, when compared with the barcodes that were dried in an open system (without glass lid). This was probably due to the slower evaporation rate of water from the ALG barcodes in the the closed system. Therefore, it could be seen from the experimental results that the structure of the barcodes could be controlled to a certain degree by indirectly slowing down the drying rate of the hydrogel barcodes.

Therefore, a qualitative interpretation of the experimental results derived from this thesis suggests that the proof of concept presented here is in the right direction towards achieving some quantitative results in the near future.

Some suggested improvements include further experimental work to optimize the current methodology as well as to observe reproducibility of the experimental protocol. Furthermore, it would be helpful to incorporate modeling to determine if there is a good fit with existing models for the drying kinetics of the system under consideration in this work. Similar suggestions are further discussed in chapter 6.

6

RECOMMENDATIONS AND LIMITATIONS

During this thesis work, much of the procedures approached were exploratory in nature, without strong predictions about the outcome. While these methods were slowly improved in minor installments, due to time constraints it was not possible to successfully implement all of the proposed ideas for refinement of the concept. Some of these are as discussed below:

1. Laser Cutting

An interesting approach that could be explored is laser cutting, and this research idea has already been initiated as seen in figure 6.1. Some promising results have been observed with laser cutting of edible sheets available in the market such as, sushi paper (Nori paper: edible seaweed sheets). It can be seen from figure 6.1a that a good result was obtained with Nori paper but the same cannot be said about the rice paper (refer figure 6.1b). However, further experiments can be conducted to observe the reproducibility of the experiments as well as study the effect of relative humidity on these thin edible sheets as discussed in detail further.

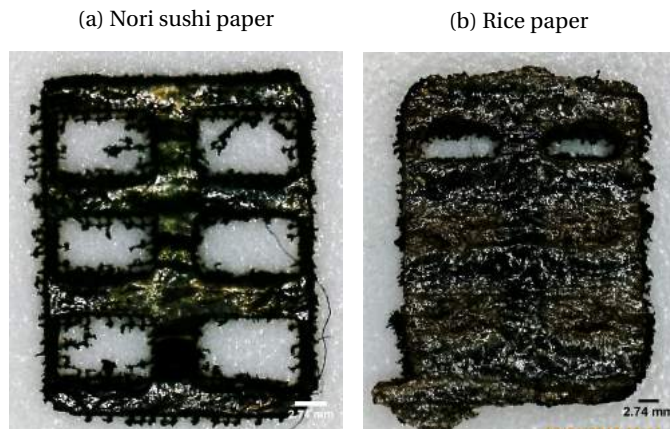


Figure 6.1: Laser cutting of edible sheets done by Jochem Meijlink³ with NEJE DK-BL Desktop Art Laser Engraver. (a) Nori shushi paper and (b) Rice paper painted black and then laser cut. Scale bar: 2.7 mm

2. Humidity chamber

In order to understand the effects of environmental conditions on the hydrogel and nori paper barcodes, a humidity chamber could be useful in terms of observing the structural changes of the barcodes with change in relative humidity with time-lapse imaging. This study could also be beneficial in developing sensory-based barcodes

³Bachelor student exploring a similar proof of principle as presented in this thesis but through a different approach, i.e., laser engraving of edible sheets

which change shape during incorrect storage, similar to the work presented by Burak and his colleagues in [1].

3. Modeling for kinetics of drying

To acquire a better understanding of the drying kinetics involved for the system under consideration, a theoretical model is required in order to fit the data available from experimental work for further validation. For example, the Page model is a common model to study the drying kinetics and literature points towards the application of such a model in the drying of hybrid carrageenans [44]. Another similar model found in literature describes the model for bead dehydration of Calcium alginate [45] which could be applied to the system in this thesis. However, an exact model to compare the current experimental data has still not been worked out due to time constraints.

4. Automation and time lapse of images during drying

The images and measurement of the dimensions of the hydrogel barcodes was done manually in this work (refer section 3.4.1). Due to this, there was difficulty in maintaining standard time intervals of images and measurement pre and post drying of all the samples. A recommendation to circumvent this issue could be by installing an oven-safe camera which will allow to view and capture images without interfering in the dynamics of the drying process [46]. This would also benefit in understanding and verifying the underlying mechanism during the drying process better. However, this could be rather expensive and complex in nature [46]. Another suggestion to improve the quantification of the dimensions of the barcodes is by ImageJ time-lapse analysis of the hydrogel barcodes during drying [47].

5. Improvement in the design of the polymer mould

Although the current design of the mould can be used and is functional in developing the hydrogel barcode and can still be used for further experiments, it could use advancement in terms of stability of the mould itself. Some of the limitations that were faced with the polymer mould include:

- Deposits on the mould can be clearly visible as seen in figure 6.2, which cannot be cleaned with ease. This implies that the mould may not be durable for a long duration and/or that frequent replacement is required.

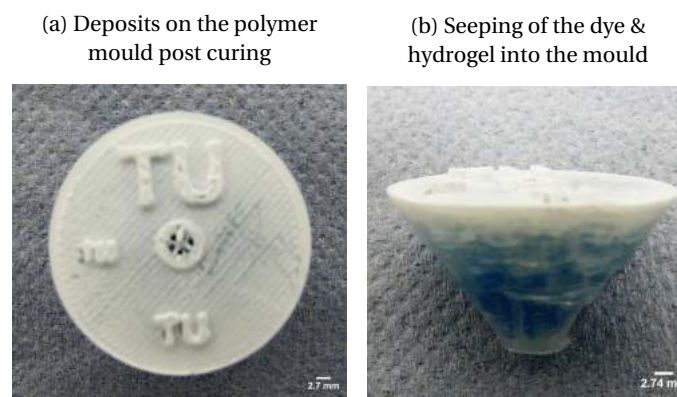


Figure 6.2: Deposits on the polymer mould due to the insolubles present in the ALG hydrogel observed post the second phase of curing. Scale bar: 2.7 mm

- The “stem” part of the mould is weak as it easily broke in the first attempt of the experimental procedure (most likely due to the weight of the hydrogel leading to a concentration of stress at the end of the stem that led to its breakage). This also makes it difficult to remove the mould itself from the falcon tube without the stem and hence, forcing the repeated use of the same falcon tube for a number of experiments. This might not be desirable considering the precision of experiments.

Therefore, it is suggested to improve this design in terms of the material used or to make enough number of replicates of the same mould. Another interesting idea could be if the mould could be designed in a manner which could be fitted into a custom made falcon tube. Probably with a click-lock mechanism at the bottom of the falcon tube (the start of the conical part) making it easier to load and unload the hydrogel onto the mould for cleaner and more precise measurements. However, research has not been done to look into these details for such a prototype.

6. TGA for ALG hydrogels made from the optimized experimental protocol

As the TGA has been performed only once for the initial experimental protocol, (where the concentration of CaCO_3 and GDL were not increased - 20 mM of CaCO_3) it is advised that the analysis be repeated to cross-check if the same trend is observed. Furthermore, in order to understand the underlying mechanisms of drying of ALG hydrogels and the governing factors that contribute to it, it would also be helpful to distinguish the trend observed from TGA conducted for the optimized experimental protocol (with increased CaCO_3 and GDL content - 40 mM of CaCO_3). Refer appendix B for the results that were obtained during this work.

7. Fixed standard precision blades for cutting

One of the difficulties faced during this work was maintaining standard dimensions of the barcode samples as they were manually cut, this ensured incorporation of certain degree of error in the measurements. To improve the standard of cutting the barcode samples, fixed cutters with varied dimensions could be used to reduce manual error and obtain cleaner measurements.

Limitations:

It is important to note the various challenges that are involved in developing the proof of concept presented in this work. To name a few, the reduction in the number of chemicals and restriction to the use of a certain class of materials contributes to the sensitivity of this process. Furthermore, handling of polymers such as alginate which are highly viscous in nature as a hydrogel is difficult, especially at higher Na-Alg concentrations making it harder to mould them into the barcodes that were required for this work. This could pose as a greater challenge ahead, should the complexity of the barcode design be increased, as would be required for the application of this concept in the market scenario.

⁴The stick that was attached to the mould as seen in figure 3.2

ACKNOWLEDGEMENTS

This thesis would be incomplete without expressing my gratitude to the people who deserve it.

I have to start by thanking my supervisor Dr.H.Burak Eral. His positivity and guidance was a constant source of motivation for me to keep pushing myself to do better. Thank you for giving me this opportunity to work in your team and helping me find an internship. But also, for having more faith in me than I did in myself. It's nice to have a teacher like you, who has taught me a lot more than just science.

I would like to also thank Prof.Dr.Antoine van der Heijden and Dr.Eduardo Mendes for taking time out of their busy schedule to be a part of my thesis committee.

I thank Johan Bijleveld for helping me with my TGA data and Spiridon van Veldhoven for 3D printing my polymer mould. I would especially also like to thank Michel van den Brink and Jaap van Raamt for always being around to help me when I needed information about anything in the labs. I thank my friend Nilesh Nahar for helping me design my 3D polymer mould as well as for all the conversations over coffee and for always telling me to aim for the top.

I would like to express my heartfelt gratitude to Rumen Georgiev for teaching me how to use the centrifuge and for always offering to help with any question that I had, science related or not. But more importantly, thank you for your suggestions on my report, for all the conversations over lunch and beer, for constantly keeping a check on my stress levels and for making sure I was sane throughout my thesis.

I thank Fatma İbiş, for helping me with the oven and for conversations over coffee and borrels. Thank you for the support and for also showing me the importance of a smile and self-composure in a working environment.

I would like to thank Dr.Erix Schokker from Friesland Campina for his support and the bachelor students who worked on the milk study project related to my topic, for providing me with the initial moulds to work with. I thank Jochem Meijlink for indirectly working alongside me and for his contribution with the laser study experiments. I thank Gabrielle Lee for supporting me during my last few weeks. I hope I have helped you with a good base to continue this work and I wish you well.

I must thank Arno Haket, my program coordinator. I would not be here, writing and defending my thesis if not for his constant source of encouragement. Thank you Arno for lifting me up during my hardest time here and not letting me quit when I so badly wanted to, several times. I will be ever grateful to you.

I thank Sameer, from the bottom of my heart for being so patient with me and my report. Thank you for being such a good friend to me.

To all the "P&E"ople (credit:Olav), also known as Burak's Army: Tom (for amusing me with all his pin-dakaas) and Roberto for checking on me time and again, but mostly for scaring me with their work ethic so I could aim to do better; Olav, for being the best lab buddy and entertainer; Sara, Yug and Yeshu, for being my pillars of support and my cheerleaders, thank you for letting me lean on you guys and for reminding me that I'm better than what I think of myself. Mehul, for being my report writing partner and whining with me, misery sure does love company; Sanan, for all the cake and Michael, for being the sweetheart that he is (that nobody else knows about).

A shout out to my extended family here at Delft, you guys are the best. Thank you for all the crazy fun. It would have been so much harder without you guys. Special thanks to Clarissa, for whining and working with me on the weekends and Shridhar, for the 'in-between thesis writing' ice cream breaks. Zoey, Mark and Sai, for being very supportive housemates. Especially Sai, thank you for keeping me alive during the last weeks of my thesis by providing home-cooked food and taking the load off. Teo, for all the love from afar and for cheering me on. Zoe, Chinmay and Rimit for allowing me to vent. Thank you Maulik, for the best advice (always) and Hongyu, for sharing my stress and laughing with me through it.

I wouldn't have grown to be the person that I am today if not for some people, who sometimes know me better than I do myself. My family from back home and afar. Suraj, Aditya, Channi, Rashmi, Mayur and Vaish,

for actually visiting me from across the globe to make sure I was doing fine. Raina, Baadi(Siddhant), Kav and Kunal, for the pep talks. Surabhi, for being my soul sister. Teji, for always telling me that “when you think life can’t get worse, it does. But that doesn’t mean that you can’t get through it”, and for defining by action what hard-work is. Alope, for all his postcards which always made me smile. A very special thank you to Arun for being the big-brother I never had, Mayur(again) for being my guardian angel and telling me to “grow up, cut the crap and suck it up”. I cannot thank you both enough.

I thank my (biological) family for being proud of me no matter what. Special mention to Mahi and Guru, for constantly checking on my well-being. Prem ,Gunmeet, Vasana Uncle and Srilatha Aunt for their love and support through numerous WhatsApp messages.

Words are not good enough to thank the next few people I’m about to mention but I’ll try. Vaishnavi, for seeing me through my darkest phase here and sticking by my side without budging. You know how much you mean to me and no words can do justice to the gratitude I have towards you. Daan, for being SO positive for me ALL the time and for giving me company when I stayed late at uni (it was never a secret!). Thorben, for being my human diary, every single day for the past year. Meera, for being my constant (literally from start to finish). You’re my person, you get me like no one else does.

Home is truly where the heart is. I thank Raghav, for knowing exactly how I feel and empathizing with me. Vinay, for being my backbone and my best friend. Your support has been unwavering and I could not have done this without you.

I thank my grandparents for being the coolest grandparents anyone could ever have and teaching us that good food, happiness and good education is the definition of good health. I dedicate this thesis to my late grandpa. I’m sorry I couldn’t be there to bid goodbye to you. I know reading this report would have given you joy, to see that I survived it. But I take comfort in knowing that you’re looking down at me with pride.

NOTHING (and I really do mean nothing) of what I have accomplished till date would have been possible if not for my sister and my parents. Thank you Amma and Appa, for making sure I got good quality education and values. Pooj, for shaping me into the best possible version of myself. Amma and Pooj, you both will forever be my role models. If I turn out to be half the person that you both are, I can say I’ve achieved something. Thank you for being crazy with me!

Last but not the least, I thank Bonobo (a.k.a Simon Green), for his music - it got me through my writing. Netflix, for providing me with reruns of E.R.I.E.N.D.S. Apart from de-stressing me, without your help I would have probably finished this thesis earlier!

Finally, I thank you, as the reader (if you have continued to keep reading) for getting through this never-ending list of acknowledgements. The past two years have been my biggest challenge yet, and I never thought I would make it to this stage. I couldn’t let go of this opportunity to express my gratitude.

BUCKLING INSTABILITY

Tanaka *et al.* state that polymer gels that are made up of a network of cross-links, when immersed in a solvent experience volume phase transition (change in volume due to swelling/shrinking), the effect of which is seen by a discontinuous, reversible shrinking or swelling of the gel [48]. The patterns thus observed appear as line segments of cusps in the gel which arise due to the shear bending of a homogeneously swollen gel surface and not due to the breaking of the shrunken segments of the gel [48]. The research also states that the pattern disappears when a thin layer of the surface is sliced off [48].

A paper by Kang and Huang imply similar observations denoting that a response to external stimuli (such as pH, Temperature, etc) [49] as well as by altering the cross-linking densities and gradients, polymeric hydrogels have the ability to undergo volume and shape changes significantly. Therefore, a variety of instability patterns can be seen because of the swelling or shrinking of hydrogels [49]. This phenomenon is particularly interesting as it finds use in many applications like microfluidic devices, controlling cellular behaviour, as adhesives and responsive coatings as well as in sensors [50]. This type of buckling instabilities can exist due to the mismatch between the bilayers inducing compressive stress which in turn activates buckling [50].

Tanaka *et al.* further explains that the kinetic process of swelling of the gel is influenced by the collective diffusion of the polymer network into a solvent and at first only a very thin layer of the surface is swollen, i.e., the layer that is subjected to mechanical constraint. However, the outer layer is unconstrained and allowed to expand rather freely, while the inner surface is secured to the core of the gel subjecting the layer to opposing constraints on the lower and upper surfaces [48]. These forces compel the layer to either swell unidirectionally perpendicular to the surface or to buckle [48]. The research also states that the characteristic wavelength of the pattern should be proportional to the thickness of the swollen layer making it the appropriate length scale taken for consideration [48].

Guvendiren *et al.* state that the buckling, creasing or the wrinkling of thin films restricted to a substrate can lead to self organized patterns within a vast span of morphology and complexity which can be controlled by altering the conformity of physical properties as well as the dimensions of the material [50]. By fine tuning this phenomenon, it can be used to make patterns useful for anti-counterfeiting purposes, one such example of this is the study of physically unclonable function based biomimetic fingerprinted taggants (where no two particles were identical) presented by Bae *et al.* [51].

While the above discussed literature is interesting, it is important to note that from the point of view of our research, the structural distortions and behaviour of hydrogels post drying after most of the solvent has been evaporated is significant to this work. Unfortunately, to the best of our knowledge, there is not enough comparable literature regarding the same. However, one such paper by Pauchard *et al.* suggests that the shape distortions that occur during the drying of sessile drops of a polymer solution is indeed due to buckling

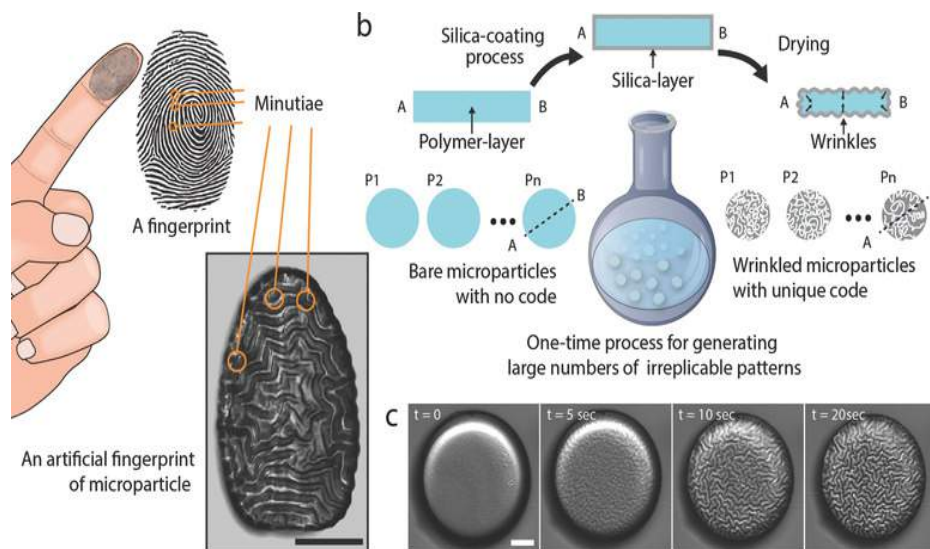


Figure A.1: Artificially fingerprinted microparticle for a biomimetic fingerprint (scale bar:50 μm). b) along with the schematic representation of the fabrication process. c) A sequence of movie frames at the wrinkling moment (scale bar:25 μm) [51].

instability [52]. Furthermore, they explain that as the solvent evaporates, there is accumulation of polymer at the vapour/drop interface and can lead to the formation of a glassy outer skin which behaves as an elastic shell that does not hinder the evaporation process. Furthermore, it tends to bend as the volume that it encloses starts to decrease [52]. Another factor that can influence the buckling instability is humidity, by altering the drying rate and the and hence the skin thickness and drying stresses [52]. Their research also throws light on the fact that microscopic phenomena such as solvent diffusion, gelation, transfers at the vapor/medium interface and specifically an increase in the concentration of non-volatile components which are factors that are responsible for the temporal and spatial alterations in structure [52].

B

THERMOGRAVIMETRIC STUDY

Thermogravimetric analysis was conducted in order to observe the change in the mass as a function of time under the influence of temperature increase, more specifically to quantify the loss of water from the hydrogel samples. The TGA for this thesis work was carried out using the PerkinElmer®TGA 4000 instrument following a temperature program that heated up the sample from 0°C to 60°C at 20°C/minute using air as the purge gas (at 20 ml/minute).

The experiment was carried out for each Na-Alg concentration of the hydrogels considered in this study to perceive a trend correlating the loss of water and the concentration of Na-Alg. The results obtained from the TGA is as seen in figure B.1 below.

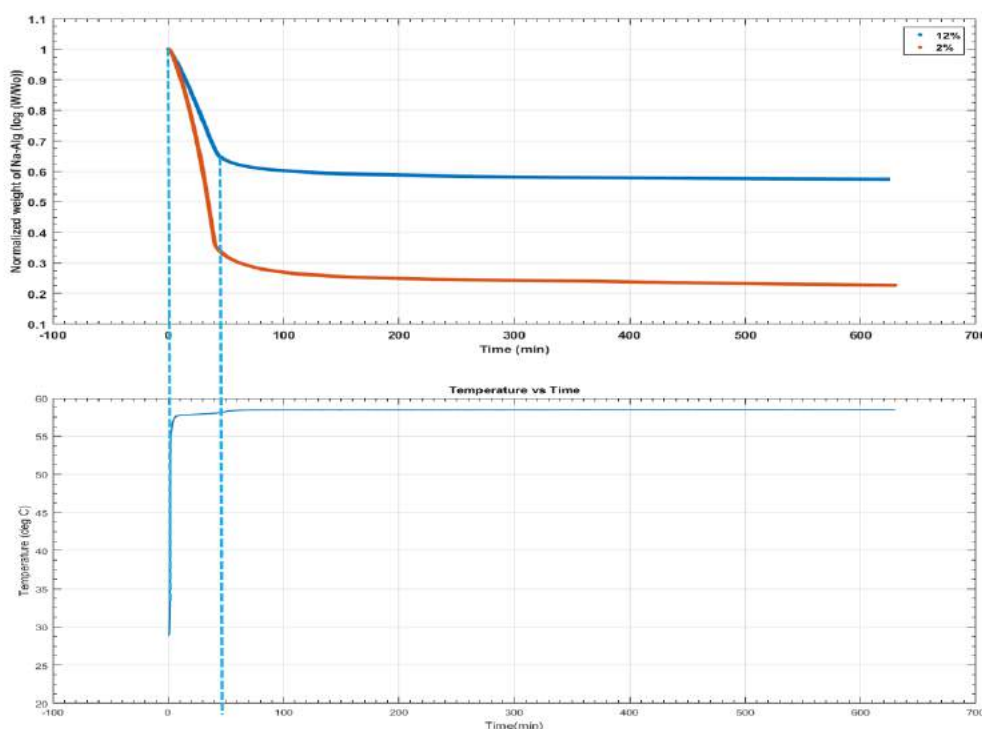


Figure B.1: TGA for 2% and 12% w/w Na-Alg in comparison to the temperature profile. Graph on top: Normalized weight of Na-Alg ($\log(w/w_0)$) vs Time (min). Bottom graph: Temperature ($^{\circ}\text{C}$) vs Time (min) from TGA

It can be seen from graph B.1 that with the steep increase in the temperature, the slope for the 2% w/w Na-Alg is steeper than for the 12% w/w Na-Alg sample. This was expected to be observed, as 12% w/w Na-Alg contains more percentage of total insolubles ($\approx 13\%$; refer appendix C for the mass balances). Therefore the rate of drying is faster as lesser

water is required to be evaporated from the hydrogel sample, when compared to the 2% w/w Na-Alg sample containing a lesser percentage of total insolubles ($\approx 5\%$; refer appendix C). Following this explanation, the same should be observed for the other concentrations of Na-Alg with decreasing value of the slope as the concentration of Na-Alg in increased. However, a trend to validate this claim could not be observed from the curves for the other concentrations of Na-Alg as seen in figure B.2.

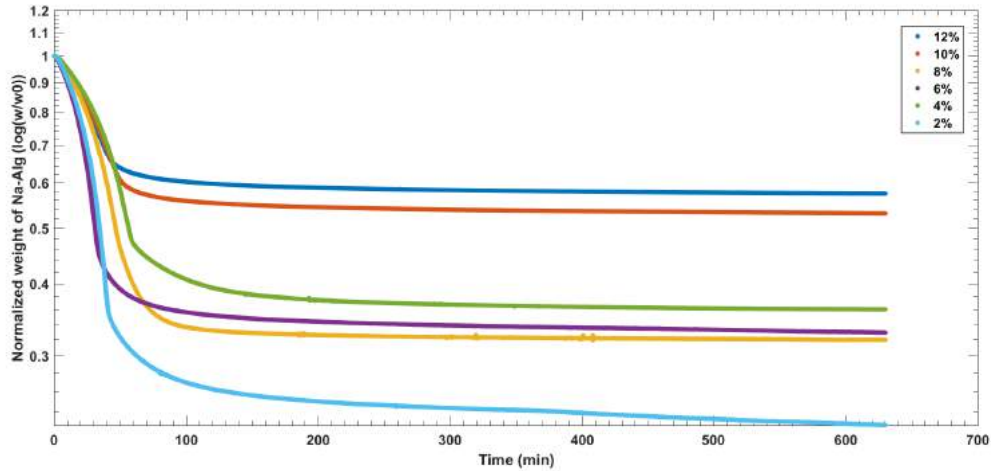


Figure B.2: TGA for all concentrations of Na-Alg (Normalized weight of Na-Alg ($\log(w/w_0)$) vs Time (min)).

If the above drying curve is compared to that of evaporation of a droplet, a single exponential decay would be observed for a curve for the the moisture retention over time [53] as predicted in figure B.3.

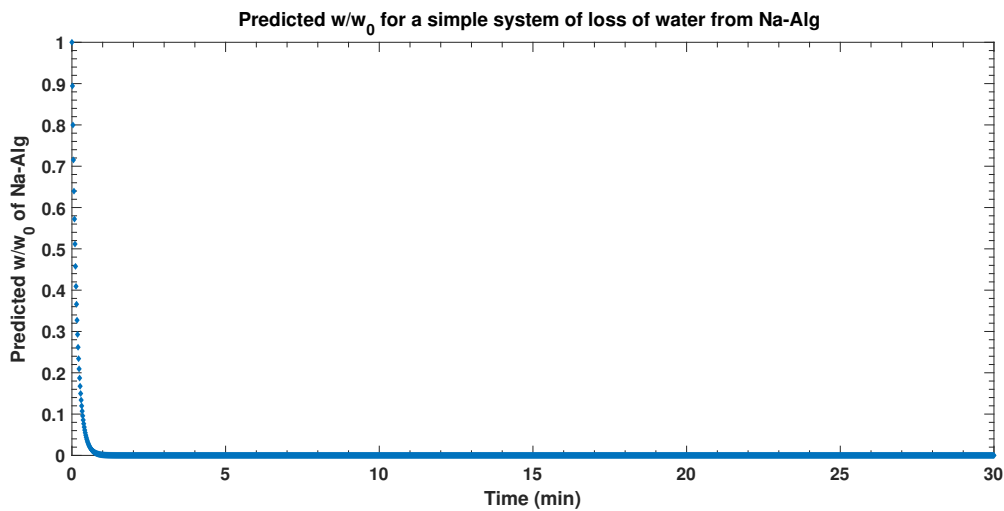


Figure B.3: Predicted curve for evaporation of water from a simple system considering only Na-Alg and water.

However, for the system under consideration in this thesis, a two-phase exponential decay trend was observed, as seen in figure B.4.

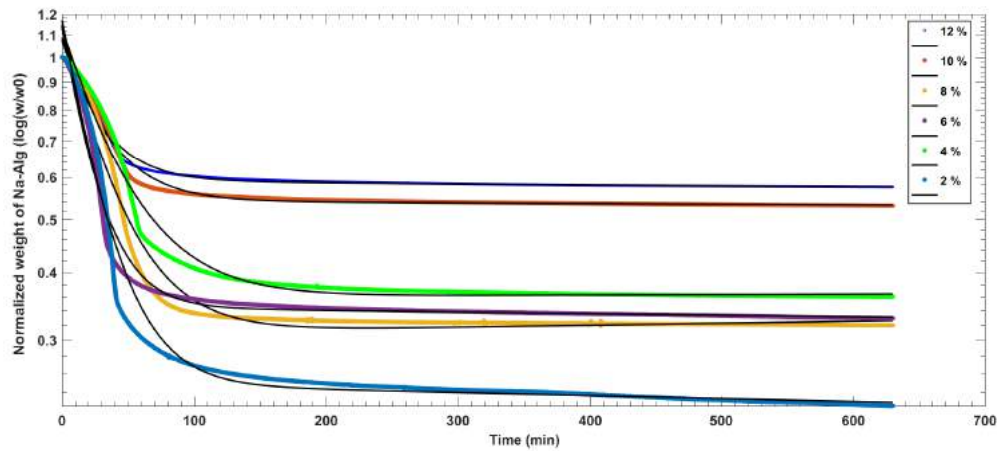


Figure B.4: Double exponential curve fit for data from TGA for all concentrations of Na-Alg (Normalized weight of Na-Alg ($\log(w/w_0)$) vs Time (min)).

The first phase could indicate the decay that is accounted for the fast time scale where the maximum loss of water trapped within the hydrogel matrix is evaporated. The second phase is depicted by a slower time scale indicating a gradual decrease in the mass of the hydrogel. This can be attributed to the remaining water content which is dried more slowly and eventually reached a constant state over a total time period of 24 hours, after which there is no more change in the mass of the hydrogel sample.

$$f(x) = a \cdot \exp(b \cdot x) + c \cdot \exp(d \cdot x)$$

where x is normalized by mean 315 and std 181.9

Coefficients (with 95% confidence bounds):

Fitting Parameters

Concentration	a	b	c	d	R-square
12% SA	4.451e-06 (4.295e-06, 4.608e-06)	-6.695 (-6.716, -6.674)	0.5818 (0.5817, 0.5819)	-0.0079 (-0.0082, -0.0078)	0.984
10% SA	1.732e-05 (1.669e-05, 1.794e-05)	-5.98 (-6.002, -5.959)	0.5366 (0.5364, 0.5367)	-0.0049 (-0.0053, -0.0047)	0.979
8% SA	7.739e-05 (7.454e-05, 8.023e-05)	-5.365 (-5.387, -5.344)	0.3172 (0.3169, 0.3175)	0.0155 (0.0145, 0.0165)	0.972
6% SA	4.794e-07 (4.542e-07, 5.045e-07)	-8.271 (-8.302, -8.24)	0.3376 (0.3374, 0.3377)	-0.0124 (-0.0130, -0.0118)	0.975
4% SA	0.0003209 (0.0003109, 0.0003308)	-4.493 (-4.511, -4.475)	0.3624 (0.3621, 0.3627)	0.0040 (0.0032, 0.0049)	0.975
2% SA	6.903e-06 (6.575e-06, 7.231e-06)	-6.813 (-6.841, -6.785)	0.2397 (0.2394, 0.2399)	-0.0229 (-0.0242, -0.0217)	0.971

Figure B.5: Fitting parameters for the double exponential curve fit for TGA data for all concentrations of Na-Alg.

As can be seen from the fitting parameters in figure B.5, there was no trend relating the drying time scale exclusively to the concentration of Na-Alg (where the parameter b gives the fast drying time scale and parameter d gives the slow drying time scale. Therefore, it can be hypothesized that there is another governing factor that is contributing and/or bringing in an additional time scale defining the process of drying of ALG hydrogels.

It is speculated that this could be due to a layer of insolubles that are forming on the hydrogel contributing to this observed trend. However, in order to reaffirm this, it is recommended that the TGA is repeated for the sake of comparison and reproducibility (refer section 6). It is also recommended that TGA be conducted for the hydrogel samples made

from the optimized experimental protocol, i.e., with an increased concentration of CaCO_3 and GDL, so as to compare and contrast the results as well as get a better understanding of the underlying mechanism showcasing the double exponential decay trend that we observe for this system.

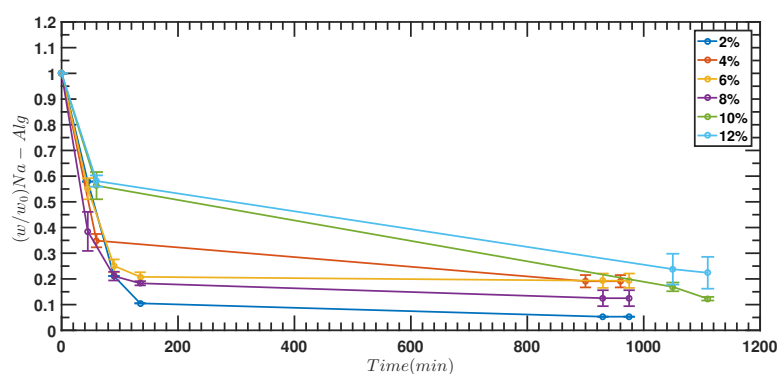
C

MASS BALANCES, SUPPLEMENTARY EXPERIMENTS & FIGURES

DRYING STUDIES

The loss of mass as a function of time for all the concentrations of Na-Alg barcode samples (with 20 mM and 40 mM of CaCO_3) when dried in the oven at 60°C was conducted as shown in figure C.1 and C.2, to validate if the concentration of Na-Alg was a prominent contributing factor to the rate of drying.

(a) Normalized weight loss of ALG vs Time for all concentrations of Na-Alg



(b) Normalized weight loss of ALG vs Time for 2% and 12% w/w Na-Alg

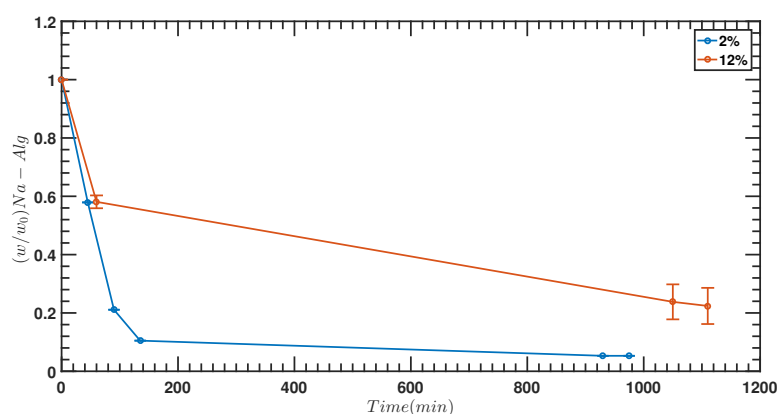
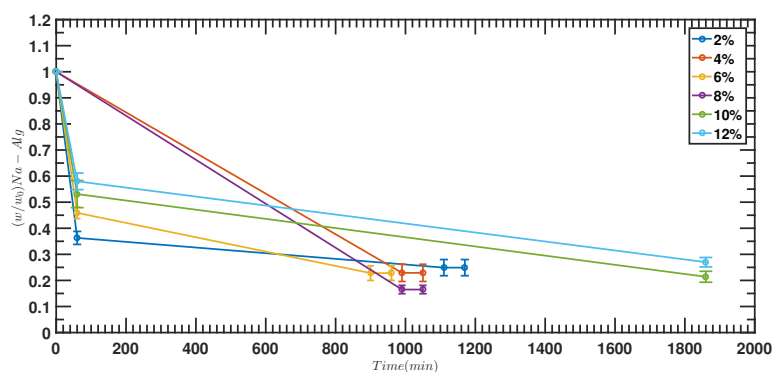


Figure C.1: Normalized weight loss of ALG vs Time (for 20 mM CaCO_3) for all concentrations of Na-Alg on drying for ≈ 24 h at 60°C

(a) Normalized weight loss of ALG vs Time for all concentrations of Na-Alg



(b) Normalized weight loss of ALG vs Time for 2% and 12% w/w Na-Alg

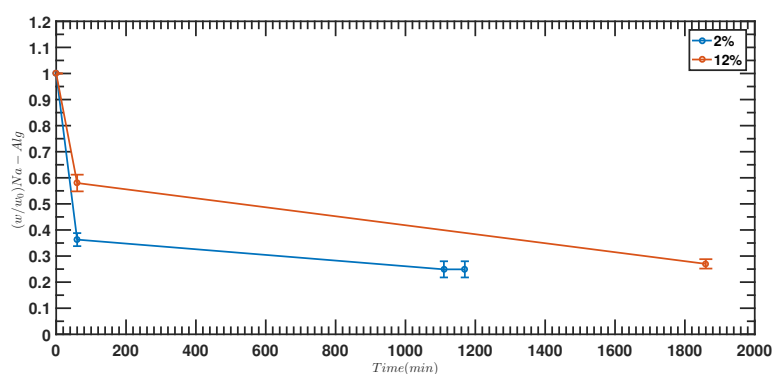


Figure C.2: Normalized weight loss of ALG vs Time (for 40 mM CaCO_3) for all concentrations of Na-Alg on drying for ≈ 24 h at 60°C

From both, figure C.1 and figure C.2, the same trend is observed with respect to the concentration of Na-Alg and hence the same conclusion holds for the above figure as that observed from TGA (refer appendix B). Although experimental error needs to be taken into consideration for the above figures, especially in figure C.2a due to less number of data points, more specifically for 4% and 6% w/w Na-Alg samples.

MASS BALANCES

A mass balance was carried out for the system under consideration. It was assumed that the mass of the insolubles remain unchanged during the process of drying and the difference in mass is accounted exclusively to the evaporation of water from the ALG hydrogel samples during the process of drying. Therefore, there is no accumulation or reaction that is taken into consideration during the drying process while carrying out this mass balance.

The mass balance was computed for TGA (refer figure C.3), ALG samples with 20 mM of CaCO₃ (refer figure C.4) as well as for the ALG samples with 40 mM of CaCO₃ (refer figure C.5) with the $[GDL]/[Ca^{2+}] = 2$ kept constant for all of the above.

From TGA						
Component	2%	4%	6%	8%	10%	12%
wi (g)	0.02312	0.04154	0.02	0.02191	0.03128	0.02714
wf (g)	0.00198	0.00379	0.0025	0.00268	0.00609	0.00648
wevap (g)	0.02114	0.03775	0.0175	0.01923	0.02519	0.02066
SA (g)	0.00044	0.0015509	0.0010995	0.0015771	0.0027647	0.0028285
NaCl (g)	0.000385	0.0006793	0.0003211	0.0003454	0.0004844	0.000413
CaCO ₃ (g)	4.4E-05	7.754E-05	3.665E-05	3.943E-05	5.529E-05	4.714E-05
GDL (g)	0.000157	0.000276	0.0001304	0.0001403	0.0001968	0.0001678
Hepes (g)	0.000105	0.0001848	8.734E-05	9.396E-05	0.0001318	0.0001123
Total Insolubles (g)	0.000691	0.0012176	0.0005755	0.0006191	0.0008682	0.0007402
% insolubles	2.986863	2.9311072	2.8773946	2.8256152	2.7756663	2.7274527
Insolubles+SA (g)	0.00113	0.0027684	0.001675	0.0021962	0.0036329	0.0035688
% Insolubles+SA	4.889082	6.6645262	8.3749006	10.023718	11.614242	13.149511
Water initial(g)	0.02199	0.0387716	0.018325	0.0197138	0.0276471	0.0235712
% water initial	95.11092	93.335474	91.625099	89.976282	88.385758	86.850489
Water final (g)	0.00085	0.0010216	0.000825	0.0004838	0.0024571	0.0029112
water lost (g)	0.02114	0.03775	0.0175	0.01923	0.02519	0.02066
% water final	42.91133	26.95398	33.000795	18.052367	40.345896	44.926275
% water lost	96.13616	97.365193	95.49785	97.545865	91.112745	87.649251
water lost/wi	0.91436	0.9087626	0.875	0.8776814	0.8053069	0.761238
% waterlost/wi	91.43599	90.876264	87.5	87.768142	80.530691	76.123803

Figure C.3: Mass balance (TGA) of different concentrations of Na-Alg

With 20mM CaCO ₃ ; [GDL]/[Ca ²⁺]=2						
Component	2%	4%	6%	8%	10%	12%
wi (g)	0.19	0.14	0.23	0.05	0.14	0.14
wf (g)	0.01	0.02	0.03	0.01	0.02	0.03
wevap (g)	0.18	0.12	0.2	0.04	0.12	0.11
SA (g)	0.003614	0.005227	0.012644	0.003599	0.012374	0.014591
NaCl (g)	0.003166	0.002289	0.003692	0.000788	0.002168	0.00213
CaCO ₃ (g)	0.000361	0.000261	0.000421	9E-05	0.000247	0.000243
GDL (g)	0.001286	0.00093	0.0015	0.00032	0.000881	0.000865
Hepes (g)	0.000861	0.000623	0.001004	0.000214	0.00059	0.00058
Total Insolubles (g)	0.005675	0.004104	0.006618	0.001413	0.003886	0.003818
% insolubles	2.986863	2.931107	2.877395	2.825615	2.775666	2.727453
Insolubles+SA (g)	0.009289	0.00933	0.019262	0.005012	0.01626	0.018409
% Insolubles+SA	4.889082	6.664526	8.374901	10.02372	11.61424	13.14951
Water initial (g)	0.180711	0.13067	0.210738	0.044988	0.12374	0.121591
% water initial	95.11092	93.33547	91.6251	89.97628	88.38576	86.85049
Water final (g)	0.000711	0.01067	0.010738	0.004988	0.00374	0.011591
water lost (g)	0.18	0.12	0.2	0.04	0.12	0.11
% water final	7.107449	53.34832	35.79243	49.88141	18.70031	38.63561
% water lost	99.60669	91.83463	94.9047	88.91232	96.97749	90.46746
water lost/wi	0.947368	0.857143	0.869565	0.8	0.857143	0.785714
% waterlost/wi	94.73684	85.71429	86.95652	80	85.71429	78.57143

Figure C.4: Mass balance (20 mM CaCO₃) of different concentrations of Na-Alg

With 40mM CaCO ₃ ; [GDL]/[Ca ²⁺]=2						
Component	2%	4%	6%	8%	10%	12%
w _i (g)	0.16	0.19	0.14	0.11	0.17	0.14
w _f (g)	0.02	0.03	0.02	0.02	0.03	0.04
w _{evap} (g)	0.14	0.16	0.12	0.09	0.14	0.1
SA (g)	0.002975	0.006936	0.007529	0.007748	0.014709	0.014289
NaCl (g)	0.002606	0.003038	0.002198	0.001697	0.002577	0.002086
CaCO ₃ (g)	0.000595	0.000694	0.000502	0.000387	0.000588	0.000476
GDL (g)	0.002117	0.002468	0.001786	0.001379	0.002094	0.001695
Hepes (g)	0	0	0	0	0	0
Indigo Carmine	0.002603	0.00292	0.002077	0.001531	0.002423	0.001701
Total Insolubles (g)	0.007921	0.00912	0.006563	0.004994	0.007682	0.005959
% insolubles	4.950565	4.800166	4.687903	4.539966	4.518825	4.256131
Insolubles+SA (g)	0.010896	0.016056	0.014092	0.012742	0.022391	0.020247
% Insolubles+SA	6.809723	8.450614	10.06542	11.58373	13.17117	14.46233
Water (g)	0.149104	0.173944	0.125908	0.097258	0.147609	0.119753
% water	93.19028	91.54939	89.93458	88.41627	86.82883	85.53767
Water final (g)	0.009104	0.013944	0.005908	0.007258	0.007609	0.019753
water lost (g)	0.14	0.16	0.12	0.09	0.14	0.1
% water final	45.52222	46.47945	29.54204	36.28947	25.36337	49.38184
% water lost	93.89392	91.98371	95.30738	92.53748	94.84516	83.5054
water lost/w _i	0.875	0.842105	0.857143	0.818182	0.823529	0.714286
% waterlost/w _i	87.5	84.21053	85.71429	81.81818	82.35294	71.42857

Figure C.5: Mass balance (40 mM CaCO₃) of different concentrations of Na-Alg

The mass balances showed that the percentage of water lost with respect to the initial water that was present in the samples was not related to the concentration of Na-Alg as expected and discussed in section 4.4. It can also be observed from figure C.6 and from figure C.7 that the percentage of water lost relative to the initial weight of the sample for all of the curves were comparable to each other. This again brings us back to the hypothesis that the insolubles present in the samples are suspected to have a prominent role in the mechanism of drying of the ALG hydrogel samples.

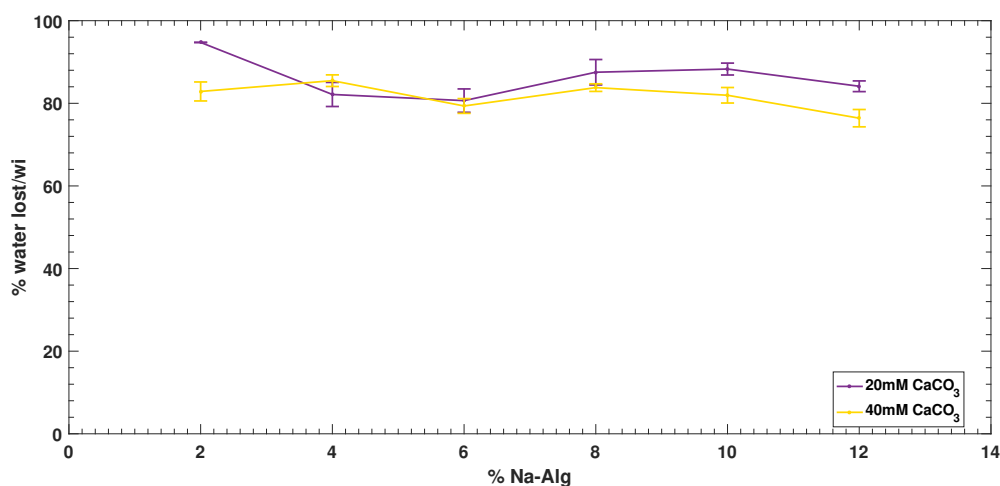


Figure C.6: Percentage of Na-Alg vs weight percentage (where w_i is the initial weight of the sample before drying) of the sample for all ALG hydrogels with varying CaCO₃ content

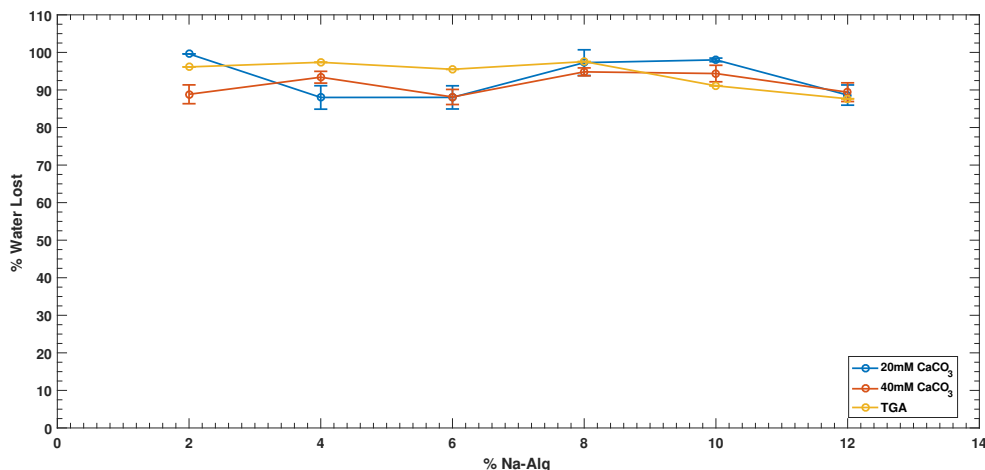


Figure C.7: Percentage of Na-Alg vs percentage of water lost for all ALG hydrogels with varying CaCO₃ content and TGA

MISCELLANEOUS ADDITIONAL EXPERIMENTS

Some additional experiments were carried out to compare which is the most suitable protocol or method for this research work.

COMPOSITE BARCODE

One such experiment was conducted by making a composite barcode out of some of the materials available in the lab such as lactose milk powder and Na-Alg.

This was done by mixing 1g of Na-Alg with 1g of lactose milk powder and 4 ml of DI water. This was mixed well manually with a stirrer and put into the rectangular metal stamper to take the shape of the “TU” barcode. The composite was left in the stamper for \approx 24 hours, after which it was pressed out of the stamper and left to dry for another 48 hours under room temperature. It was observed that this composite also took the imprint of the barcode, however a clean barcode could not be fabricated in this method due to difficulty of uniform mixing as seen in figure C. Hence, this experimental idea was not carried forward any further.



Figure C.8: Composite barcode made from lactose milk powder and Na-Alg

METAL STAMPER TESTS

The first moulds used for making the hydrogel barcodes were the metal stampers, but as discussed in detail in section 4.1.1, one or more of the components used in making the hydrogel reacted with the metal and thus interfering with the curing of the hydrogel. Therefore, in order to verify which of the individual components used in the experimental protocol had a reaction with the circular metal stamper (made from aluminium) the most, the metal stamper was allowed to rest in a solution of each of the individual components used in the experimental protocol for ≈ 24 hours each, in the order that they were added. That is, the metal stamper was immersed in a 1% w/w solution of NaCl in DI water, similarly for Na-Alg, CaCO_3 , GDL and finally hepes.

From this simple test and figure C, it was observed that CaCO_3 reacted most with the material of the metal stamper than the other components used to make the hydrogel barcodes. As also observed for the polymer moulds as described in section 6.



Figure C.9: Metal stamper test results showing deposits of CaCO_3 . Scale bar corresponds to 2.7 mm

It is therefore, important to note that care must be taken when selecting the material of the mould for curing/developing the hydrogel barcodes so as to avoid or reduce the occurrence of deposits.

BIBLIOGRAPHY

- [1] I. Rehor, S. van Vreeswijk, T. Vermonden, W. E. Hennink, W. K. Kegel, and H. B. Eral, *Biodegradable Microparticles for Simultaneous Detection of Counterfeit and Deteriorated Edible Products*, [Small](#) , 1701804 (2017).
- [2] C. K. Kuo and P. X. Ma, *Ionicly crosslinked alginate hydrogels as scaffolds for tissue engineering: Part 1. Structure, gelation rate and mechanical properties*, [Biomaterials](#) **22**, 511 (2001), NIHMS150003 .
- [3] W. H. Organization, *Substandard, spurious, falsely labelled, falsified and counterfeit(ssffc) medical products*, (2018).
- [4] C. Sumners, *Drug stability: How storage conditions affect their performance*, (2016).
- [5] I. P. Federation, *Fip combats falsified and substandard medicines*, (2018).
- [6] N. Christian Purefoy of CNN, Lagos, *Poisoned medicine kills dozens of children in nigeria*, (2008).
- [7] A. Press, *China top food safety official resigns*, (2008).
- [8] T. N. I. for Occupational Safety and H. (NIOSH), *Melamine*, (2015).
- [9] H. Xin and R. Stone, *Tainted milk scandal: Chinese probe unmasks high-tech adulteration with melamine*, [Science](#) **322**, 1310 (2008).
- [10] G. Power, *Anti-counterfeit Technologies for the Protection of Medicines*, IMPACT - World Health Organisation Report , 1 (2008).
- [11] WHO, *International Medical Products Anti-Counterfeiting Taskforce (IMPACT)* (2010) pp. 1–164.
- [12] G. Gabriels, M. Lambert, P. Smith, L. Wiesner, and D. Hiss, *Melamine contamination in nutritional supplements - Is it an alarm bell for the general consumer, athletes, and 'Weekend Warriors'?* [Nutrition Journal](#) **14**, 1 (2015).
- [13] J. V. der Ploeg, *Exporting baby milk powder to china rises spectacularly*, (2015).
- [14] M. You, M. Lin, S. Wang, X. Wang, G. Zhang, Y. Hong, Y. Dong, G. Jin, and F. Xu, *Three-dimensional quick response code based on inkjet printing of upconversion fluorescent nanoparticles for drug anti-counterfeiting*, [Nanoscale](#) **8**, 10096 (2016).
- [15] J. Fei and R. Liu, *Drug-laden 3D biodegradable label using QR code for anti-counterfeiting of drugs*, [Materials Science and Engineering C](#) **63**, 657 (2016).
- [16] Y. He, F. Yang, H. Zhao, Q. Gao, B. Xia, and J. Fu, *Research on the printability of hydrogels in 3D bioprinting*, [Scientific Reports](#) **6**, 29977 (2016).

- [17] E. Axpe and M. L. Oyen, *Applications of Alginate-Based Bioinks in 3D Bioprinting*, [International journal of molecular sciences](#) **17** (2016), 10.3390/ijms17121976.
- [18] B. Duong, H. Liu, C. Li, W. Deng, L. Ma, and M. Su, *Printed multilayer microtaggants with phase change nanoparticles for enhanced labeling security*, [ACS Applied Materials and Interfaces](#) **6**, 8909 (2014).
- [19] A. Czarnik, *Encoding methods for combinatorial chemistry*, [Current Opinion in Chemical Biology](#) **1**, 60 (1997).
- [20] J. L. Kiel, E. A. Holwitt, J. E. Parker, J. Vivekananda, V. Franz, M. A. Sloan, A. W. Miziolek, F. C. DeLucia Jr., C. A. Munson, and Y. D. Mattley, *Specific biological agent taggants*, [Proceedings of SPIE - The International Society for Optical Engineering](#) **5795**, 39 (2005).
- [21] C. T. Clelland, V. Risca, and C. Bancroft, *Hiding messages in DNA microdots*, [Nature](#) **399**, 533 (1999).
- [22] SafeTracesInc, *First dna-based traceability system delivered to secure fertilizer production*, (2018).
- [23] TruTagTechnologies, *Brand protection - trutag microtags*, (2016).
- [24] Taaneh.com, *The taaneh solution to counterfeiting*, (2015).
- [25] A. Zografos and G. R. Farquar, *Dna based bar code for improved food traceability*, (2015).
- [26] SafeTraces.com, *Verify food source and purity in minutes*, (2018).
- [27] I. Recommendations, *Compendium of polymer terminology and nomenclature*, Prepared for publication by RG Jones, J. Kahovec, R. Stepto, ES Wilks, M. Hess, T. Kitayama, WV Metanowski, with advice from A. Jenkins and P. Kratochvil, RSC Publishing, Cambridge, UK (2008). Google Scholar (2008).
- [28] R. J. Young and P. A. Lovell, *Introduction to polymers* (CRC press, 2011).
- [29] F. Vert, M.; Doi, Y.; Hellwich, K.; Hess, M.; Hodge, P.; Kubisa, P.; Rinaudo, M.; Schue, *Terminology for biorelated polymers and applications (IUPAC Recommendations 2012)*, [Pure Appl. Chem.](#) **84**, 377 (2012).
- [30] K. Y. Lee and D. J. Mooney, *Alginate: properties and biomedical applications*, [Progress in polymer science](#) **37**, 106 (2012).
- [31] S. Gulrez, S. Al-Assaf, and G. O. Phillips, *Hydrogels : Methods of Preparation , Characterisation and Applications*, [Progress in Molecular and Environmental Bioengineering](#) **51**, 117 (2003).
- [32] W. E. Hennink and C. F. van Nostrum, *Novel crosslinking methods to design hydrogels*, [Advanced Drug Delivery Reviews](#) **64**, 223 (2012).
- [33] S. J. Buwalda, K. W. Boere, P. J. Dijkstra, J. Feijen, T. Vermonden, and W. E. Hennink, *Hydrogels in a historical perspective: From simple networks to smart materials*, [Journal of Controlled Release](#) **190**, 254 (2014), arXiv:NIHMS150003 .

- [34] G. A. Paleos, *What are hydrogels*, Retrieved October 11, 2015 (2012).
- [35] M. F. Akhtar, M. Hanif, and N. M. Ranjha, *Methods of synthesis of hydrogels... A review*, *Saudi Pharmaceutical Journal* **24**, 554 (2016), [arXiv:0410550 \[cond-mat\]](#) .
- [36] J. Berger, M. Reist, J. M. Mayer, O. Felt, N. A. Peppas, and R. Gurny, *Structure and interactions in covalently and ionically crosslinked chitosan hydrogels for biomedical applications*, *European Journal of Pharmaceutics and Biopharmaceutics* **57**, 19 (2004), [arXiv:9809069v1 \[arXiv:gr-qc\]](#) .
- [37] U. Food and D. Administration, *Generally recognised as safe-gras*, (1958).
- [38] A. D. Augst, H. J. Kong, and D. J. Mooney, *Alginate hydrogels as biomaterials*, *Macromolecular Bioscience* **6**, 623 (2006).
- [39] D. E. Clark, H. C. Green, and C. Kelco, *United states 2,036,922*, (1936).
- [40] K. I. Draget, O. Smidsrød, and G. Skjåk-Bræk, *Biopolymers Online*, January (2005).
- [41] H. B. Eral, V. López-Mejías, M. O'Mahony, B. L. Trout, A. S. Myerson, and P. S. Doyle, *Biocompatible alginate microgel particles as heteronucleants and encapsulating vehicles for hydrophilic and hydrophobic drugs*, *Crystal Growth and Design* **14**, 2073 (2014).
- [42] J. Boelhouwers, J. Bender, M. Damoiseaux, and J. Lardinois, *eBarcodes: Edible multifunctional barcodes*, Bachelor's thesis, Delft University of Technology, The Netherlands (2017).
- [43] H. F. Acid, *HEPES FREE ACID Sigma Prod. Nos. H3375, H7523, H6147, H9136 and H4034*, *Microscopy* , 5.
- [44] S. Arufe, M. D. Torres, F. Chenlo, and R. Moreira, *Air drying modelling of mastocarpus stellatus seaweed a source of hybrid carrageenan*, *Heat and Mass Transfer* **54**, 177 (2018).
- [45] M. E. Lyn and D. Ying, *Drying model for calcium alginate beads*, *Industrial & engineering chemistry research* **49**, 1986 (2010).
- [46] R. C. Pfaffinger, M. A. Funk, R. L. Tyler, *et al.*, *Oven camera assembly*, (2017), uS Patent 9,615,007.
- [47] W. R. T. Ferreira, *ImageJ User Guide IJ 1.46r, IJ 1.46r* , 185 (2012), [arXiv:1081-8693](#) .
- [48] T. Tanaka, S.-T. Sun, Y. Hirokawa, S. Katayama, J. Kucera, Y. Hirose, and T. Amiya, *Mechanical instability of gels at the phase transition*, (1987).
- [49] M. K. Kang and R. Huang, *Swell-induced surface instability of confined hydrogel layers on substrates*, (2010).
- [50] M. Guvendiren, S. Yang, and J. A. Burdick, *Swelling-Induced surface patterns in hydrogels with gradient crosslinking density*, *Advanced Functional Materials* **19**, 3038 (2009).
- [51] H. J. Bae, S. Bae, C. Park, S. Han, J. Kim, L. N. Kim, K. Kim, S. H. Song, W. Park, and S. Kwon, *Biomimetic microfingerprints for anti-counterfeiting strategies*, *Advanced Materials* **27**, 2083 (2015).

-
- [52] L. Pauchard and C. Allain, *Buckling Instability induced by polymer solution drying*, [EPL \(Europhysics Letters\)](#) **62**, 893 (2003).
- [53] X. D. Chen and A. S. Mujumdar, *Drying technologies in food processing* (John Wiley & Sons, 2009) pp. 8–9.